Cellular/Molecular

Voltage-Gated Na$^+$ Channel β1B: A Secreted Cell Adhesion Molecule Involved in Human Epilepsy

Gustavo A. Patino,[1] **William J. Brackenbury,**[1] **Yangyang Bao,**[1] **Luis F. Lopez-Santiago,**[1] **Heather A. O'Malley,**[1] **Chunling Chen,**[1] **Jeffrey D. Calhoun,**[2] **Ron G. Lafrenière,**[3,5] **Patrick Cossette,**[4,6] **Guy A. Rouleau,**[3,5] **and Lori L. Isom**[1,2]

[1]Department of Pharmacology and Program in Neuroscience, and [2]Cellular and Molecular Biology Program, University of Michigan Medical School, Ann Arbor, Michigan 48109, [3]Centre of Excellence in Neuromics and [4]Department of Medicine, Université de Montréal, Montréal, Québec H2L 2W5, Canada, [5]Emerillon Therapeutics, Inc., Montréal, Québec H3A IL2, Canada, and [6]Centre Hospitalier de l'Université de Montréal–Hôpital Notre-Dame, Montréal, Québec H2L 4M1, Canada

Scn1b-null mice have a severe neurological and cardiac phenotype. Human mutations in *SCN1B* result in epilepsy and cardiac arrhythmia. *SCN1B* is expressed as two developmentally regulated splice variants, β1 and β1B, that are each expressed in brain and heart in rodents and humans. Here, we studied the structure and function of β1B and investigated a novel human *SCN1B* epilepsy-related mutation (p.G257R) unique to β1B. We show that wild-type β1B is not a transmembrane protein, but a soluble protein expressed predominantly during embryonic development that promotes neurite outgrowth. Association of β1B with voltage-gated Na$^+$ channels Na$_v$1.1 or Na$_v$1.3 is not detectable by immunoprecipitation and β1B does not affect Na$_v$1.3 cell surface expression as measured by [^{3}H]saxitoxin binding. However, β1B coexpression results in subtle alteration of Na$_v$1.3 currents in transfected cells, suggesting that β1B may modulate Na$^+$ current in brain. Similar to the previously characterized p.R125C mutation, p.G257R results in intracellular retention of β1B, generating a functional null allele. In contrast, two other *SCN1B* mutations associated with epilepsy, p.C121W and p.R85H, are expressed at the cell surface. We propose that β1B p.G257R may contribute to epilepsy through a mechanism that includes intracellular retention resulting in aberrant neuronal pathfinding.

Introduction

SCN1B is essential for life. Deletion of *Scn1b* in mice results in epilepsy, ataxia, growth retardation, cardiac abnormalities, and death (Chen et al., 2004; Lopez-Santiago et al., 2007). Human mutations in *SCN1B* result in genetic epilepsy with febrile seizures plus (GEFS+) spectrum disorders (Scheffer et al., 2007; Patino and Isom, 2010), Brugada syndrome (Watanabe et al., 2008), and atrial fibrillation (Watanabe et al., 2009). Patients

carrying two alleles of a *SCN1B* functional null mutation, p.R125C, have Dravet syndrome, a pediatric encephalopathy associated with mental retardation that is the most severe GEFS+ spectrum disease (Patino et al., 2009). *SCN1B* is expressed as two splice variants, β1 and β1B (originally called β1A) that includes a retained intron encoding a novel C terminus, stop codon, and polyadenylation site (Kazen-Gillespie et al., 2000; Qin et al., 2003). Both β1 and β1B are expressed in human brain and heart. β1 functions in current modulation, channel expression and subcellular localization, cell–cell adhesion, cellular migration, and neurite outgrowth (Brackenbury et al., 2008a,b). In contrast, little is known about the function of β1B. Because *Scn1b*-null mice lack both splice variants, some aspects of their phenotype may be due to the absence of β1B; however, this has not been investigated. Because all of the *SCN1B* epilepsy mutations thus far are located in the Ig domain region common to both variants (Patino et al., 2009), β1B, as well as β1, is likely involved in human brain disease. Our goal here was to understand the structure and function of β1B and to investigate a novel human *SCN1B* mutation (p.G257R) located in the region unique to β1B. We demonstrate that β1B is not a transmembrane protein but is a soluble protein that functions as a ligand for β1-mediated neurite outgrowth. While all four β-subunit genes have a similar exon–intron structure, only *SCN1B* appears to encode variants generated by alternate splicing, with variants that include two different retained introns (Oh and Waxman, 1994; Dib-Hajj and Waxman, 1995; Kazen-Gillespie et al., 2000), suggesting complex gene regulation. β1B is expressed predominantly during embryonic brain devel-

opment, with the ratio of $\beta1{:}\beta1B$ mRNA increasing into adulthood, when $\beta1$ becomes the major splice variant. Association of $\beta1B$ with voltage-gated Na$^+$ channel (VGSC) α-subunits was not detected. However, $\beta1B$ coexpression results in subtle modulation of Na$_v1.3$-generated Na$^+$ current, suggesting that this may occur in brain. Consistent with its predicted role as a cell adhesion molecule (CAM), $\beta1B$ stimulates neurite outgrowth through adhesion with neuronal $\beta1$-subunits. These results support the idea that SCN1B encoded β-subunits are key players in brain development with functions that may be unrelated to channel modulation. p.G257R results in intracellular retention of $\beta1B$, generating a functional null allele. We conclude that $\beta1B$ is a secreted CAM, expressed predominantly in embryonic brain, which stimulates neurite outgrowth. We hypothesize that the p.G257R mutation may be a risk factor for epilepsy through a mechanism that includes intracellular retention of $\beta1B$, resulting in aberrant neuronal migration and/or pathfinding, leading to changes in excitability.

Materials and Methods

Animals. Scn1b wild-type and null mice of either sex, congenic on the C57BL/6 background for at least 18 generations, were generated from Scn1b$^{+/-}$ mice as described previously (Chen et al., 2004). Animals were housed in the Unit for Laboratory Animal Medicine at the University of Michigan. All procedures were performed in accordance with University of Michigan guidelines for animal use and care.

Antibodies. Primary antibodies were as follows: anti-V5 monoclonal antibody (1:1000; AbD Serotec; MCA1360, used for Western blotting; or 1:200; Invitrogen; R960-25, used for immunofluorescence), mouse or rabbit anti-pan-VGSC antibodies (1:1000; Sigma-Aldrich; S8809 or S6936, respectively), anti-protein disulfide isomerase (PDI) (1:400; Abcam), Alexa 488-conjugated goat anti-human IgG, Fcγ fragment (1:500; Jackson ImmunoResearch), and anti-Na$^+$/K$^+$ ATPase $\beta1$-subunit antibody (1:2000; Thermo Fisher Scientific; MA1-16732). The specificity of the anti-V5 antibody in 1610 and HEK cells has been reported previously (Patino et al., 2009). Secondary antibodies were as follows: for Western blots, HRP-conjugated goat anti-rabbit or anti-mouse, diluted 1:2000 (Pierce); for immunofluorescence, goat anti-mouse or anti-rabbit secondary antibody coupled to Alexa 488 or 594 (Invitrogen), diluted 1:500.

Reverse-transcriptase PCR. Fetal frontal lobe total RNA samples (22 and 36 week gestation) were obtained from AMS Biotechnology. Postnatal frontal lobe ($n = 4$) and occipital lobe ($n = 4$) total RNA samples were kindly provided by Dr. Miriam Meisler (Department of Human Genetics, University of Michigan, Ann Arbor, MI). Total brain RNA samples from SCN1B-null mice were used as negative controls. The reverse transcriptase-PCR (RT-PCR) mix was prepared using 0.5 μg of RNA as template and the Titan One Tube RT-PCR System (Roche) according to the manufacturer's instructions. The forward primer was the same for the amplification of both $\beta1$ and $\beta1B$: 5′-GTC GTC AAG AAG ATC CAC ATT GAG GT-3′. The reverse primer for $\beta1$ was 5′-TTC GGC CAC CTG GAC GCC CGT GCA G-3′ and, for $\beta1B$, was 5′-AAC CAC ACC CCG AGA AAC ACA TCG GA-3′. Steps of the RT-PCR were as follows: 50°C for 40 s, 94°C for 2 min, 30 cycles of the following: 94°C for 15 s, 65°C for 30 s, 68°C for 1 min; and then 70°C for 7 min. The forward and reverse primers for $\beta1$ were 88.5 and 88% conserved, respectively. Because the sequence of $\beta1B$ is species specific, there was little to no conservation between species in this region.

Quantitative PCR. Custom TaqMan MGB probes were ordered from Applied Biosystems. For $\beta1$ (product number 4331348; AILIWI2), the forward primer was 5′-GGC AGA GAT GAT TTA CTG CTA CAA GA-3′, the reverse primer was 5′-GAG GTG ATG GCC AGG TAT TCC-3′, and the probe primer was 5′-CCG CCA CGG AGA CTG-3′. For $\beta1B$ (product number 4331348; AIMRUPA), the forward primer was 5′-TCC TGC CCA CTC CAG CT-3′, the reverse primer was 5′-GGG ACA GGC ATG CTT TGA C-3′, and the probe primer was 5′-CTG GCC TCT GTT TCT C-3′. Equivalent efficiency of both sets of primers was confirmed by extracting RNA from 1610-$\beta1V5$ cells coexpressing $\beta1B$ in p.TRACER

Table 1. PCR primers used to amplify regions of the human SCN1B gene

Exon	Forward primer sequence (5′ > 3′)	Reverse primer sequence (5′ > 3′)	Size (bp)
1	CGCGCTCCCGGGGACATTCTAACC	CCCGGCCCCCACCCGCTGGAG	356
2	CAATGGGTGCCTCTGCCTGAC	CCCACCGCCTCCCACTCGT	269
3A^a	GAGAGGCCCAGGCAGTGACA	GTTCTGTACCCGGAGCGTCTGT	527
3B^a	CAGCCCCTTCCTGCCCACTCC	CCCGCCCCAGAGGTGTTGAG	465
4	GAGGGCCTCCAGAATGACACAGAT	CGGGCTCCGGAGTTCCTCTC	440
5	GGGGTTGGGTCGGTCTGATGATGG	AGGGCCTGAAGGGGAGCAAGAGA	222
6	GCCGAAGTCCCCCAGGTCCCTAAT	AGGAGCTGGAGGAGGCGAAAGTGG	233

For details on the PCR protocols used for amplification, see Materials and Methods.
^{a}Exon 3 was amplified in two separate minimally overlapping PCR fragments.

using Trizol (Invitrogen) according to the manufacturer's instructions. cDNA was synthesized from the extracted RNA as described below and dilutions made over a range of 5-log. Diluted cDNA was then used to perform TaqMan Gene Expression Assays in a StepOnePlus Real-Time PCR System with TaqMan Gene Expression Master Mix (both from Applied Biosystems) according to the manufacturer's instructions. C_T determinations were made with the StepOne software, version 2.0 (Applied Biosystems), and used to calculate the efficiency of each primer pair. There was no statistical difference between the efficiencies of both sets of primers. Six micrograms of each sample of human RNA were incubated with DNase I (Invitrogen) following the manufacturer's instructions. cDNA was then synthesized using the SuperScript First-Strand System (Invitrogen) according to the instructions of the manufacturer. The final volume of cDNA was then divided in 2 (for the $\beta1$ and $\beta1B$ assays, respectively) and used as template for the TaqMan Gene Expression Assay using the standard cycling program. At least five repeats for each RNA sample were obtained. C_T values were then used to calculate mean C_T and SD for each sample. From the mean C_T values, $2^{-\Delta CT}$ were calculated for every developmental stage and SD calculated as the square root $((SD$ of $\beta1\ C_T)^2 + (SD$ of $\beta1B\ C_T)^2)$.

In silico prediction of transmembrane domains and amino acid sequence alignment. Amino acid sequences of human $\beta1$ (NP_001028.1), human $\beta1B$ (NP_950238.1), rat $\beta1$ (NP_058984.1), rat $\beta1B$ (AAF25186.1), and mouse $\beta1$ (NP_035452.1) were obtained from NCBI. The N-terminal region of mouse $\beta1/\beta1B$, encoded by the first three exons of Scn1b, was obtained by aligning the mouse $\beta1$ sequence with those of the human and rat and comparing the common region to mouse chromosome 7 (AC158993.2). The unique C-terminal region of mouse $\beta1B$ was obtained by translating the third intron of mouse Scn1b in the chromosome 7 sequence. The mouse $\beta1B$ amino acid sequence used for analysis was the composite of the resulting N- and C-terminal sequences. To predict transmembrane domains, $\beta1$ and $\beta1B$ amino acid sequences were analyzed using the Goldman Engelman Steitz hydrophobicity scale, with a certain cutoff value of 1.0 and a putative cutoff value of 0.6, using Top-Pred software (http://mobyle.pasteur.fr/cgi-bin/portal.py?form=toppred; Institut Pasteur) (von Heijne, 1992; Claros and von Heijne, 1994). Alignment of human, mouse, and rat $\beta1$ and $\beta1B$ amino acid sequences was performed using CLUSTALW software at the Pôle Bioinformatique Lyonnais (http://npsa-pbil.ibcp.fr/cgi-bin/npsa_automat.pl?page=npsa_clustalw.html), using default settings (Thompson et al., 1994).

Expression vectors and site-directed mutagenesis. The plasmid $\beta1V5$ contains a C-terminal V5-His-epitope tag and has been described previously (Patino et al., 2009). The cDNA for human $\beta1B$ was amplified by PCR and ligated into pTRACER-CMV2 (Invitrogen) at the EcoRI restriction site. The p.G257R mutation was introduced by site-directed mutagenesis using the QuikChange II kit (Stratagene). V5-His epitope tags were added to the C termini of $\beta1B$ and $\beta1B$ p.G257R cDNAs using a PCR strategy followed by ligation into pcDNA3.1/V5-His TOPO TA (Invitrogen). $\beta1V5$ and $\beta1BV5$ cDNAs were subcloned into pcDNA3.1 Hygro (+) to facilitate generation of stable cell lines. The p.R214Q, p.S248R, and p.R250T mutations were introduced into $\beta1BV5$ cDNA in pcDNA3.1/V5-His by site-directed mutagenesis using the QuikChange II kit. A similar strategy was used to introduce the p.C121W and p.R85H mutations into $\beta1V5$ cDNA in pcDNA3.1/V5-His. We previously described $\beta1Fc$, a recombinant, secreted molecule containing the $\beta1$ extracellular domain fused to the Fc region of human IgG1 (McEwen and

Table 2. Touchdown PCR amplification conditions

		Touchdown				Amplification				
Protocol	Initial denaturation (1 cycle)	Denaturation temperature (30 s)	Annealing temperature ramp (30 s)	Elongation temperature (45 s)	Cycles	Denaturation temperature (30 s)	Annealing temperature (30 s)	Elongation temperature (45 s)	Cycles	Final elongation (1 cycle)
TD1	94°C, 4 min	94°C	70–53°C (−1°C per cycle)	72°C	17	94°C	54°C	72°C	25	72°C, 5 min
TD3	94°C, 4 min	94°C	70–60°C (−1°C per cycle)	72°C	10	94°C	60°C	72°C	30	72°C, 5 min
TD8	94°C, 4 min	94°C	66–59°C (−0.5°C per cycle)	72°C	14	94°C	58°C	72°C	25	72°C, 5 min
TD10	94°C, 4 min	94°C	70–63°C (−0.5°C per cycle)	72°C	14	94°C	62°C	72°C	25	72°C, 5 min
TD11	94°C, 4 min	94°C	72–65°C (−0.5°C per cycle)	72°C	14	94°C	64°C	72°C	25	72°C, 5 min

Isom, 2004). To generate a stable β1Fc-producing cell line, cDNA encoding the extracellular domain of rat *Scn1b* was ligated into pINFUSE-hIgG1-Fc1 (Invitrogen). The integrity of all plasmids was confirmed by DNA sequencing at the University of Michigan DNA Sequencing Core. PCR primers and conditions for all reactions are available upon request. The cDNA for human Na$_v$1.5 corresponding to the hH1 polymorphism (GenBank accession number M77235) (Makielski et al., 2003) in pRc-CMV (Invitrogen) was provided by Dr. Al George (Division of Genetic Medicine and Vanderbilt Institute for Integrative Genomics, Vanderbilt University, Nashville, TN).

Cell lines. All cell lines were maintained at 37°C with 5% CO$_2$. Chinese hamster lung 1610 cells stably transfected with Na$_v$1.5 (1610hNa$_v$1.5), β1V5, or β1BV5 were cultured in DMEM with low glucose, L-glutamine, and sodium pyruvate supplemented with 5% heat-inactivated fetal bovine serum (HI-FBS), 100 U plus 100 μg/ml penicillin/streptomycin, 400 μg/ml (2R,3S,4R,5R,6S)-5-amino-6-[(1R,2S,3S,4R,6S)-4,6-diamino-3-[(2R,3R,4R,5R)-3,5-dihydroxy-5-methyl-4-methylaminooxan-2-yl]oxy-2-hydroxycyclohexyl]oxy-2-(1-hydroxyethyl)oxane-3,4-diol (G418), and 0.25 μg/ml Fungizone (all from Invitrogen). HEK-293 cells expressing human Na$_v$1.1 (GenBank accession number NP_008851.3; HEKhNa$_v$1.1) were obtained from GlaxoSmithKline under a materials transfer agreement and maintained in DMEM supplemented with 10% HI-FBS, 400 μg/ml G418, 1% nonessential amino acids, 100 U plus 100 μg/ml penicillin/streptomycin, and 0.25 μg/ml Fungizone. Chinese hamster ovary cells stably expressing human Na$_v$1.3 (GenBank accession number NP_008853.3; CHOhNa$_v$1.3) were provided by Dr. David Ragsdale (Montreal Neurological Institute, Montreal, QC, Canada) and maintained in 1× Iscove's modified Dulbecco's medium with L-glutamine and 25 mM HEPES, supplemented with 10% HI-FBS, 400 μg/ml G418, 1% nonessential amino acids, 100 U plus 100 μg/ml penicillin/streptomycin, and 1% HT supplement (Invitrogen).

For transient transfection of HEKhNa$_v$1.1 cells (Fugene 6; Roche), 7.5 μg of cDNA encoding β1V5 or β1BV5 were used. Twenty-four to 48 h later, cells were collected for experiments.

To generate stable cell lines, 2.5 μg of β-subunit cDNAs were transfected (Fugene 6), and 24 h later cells were passaged into fresh medium containing selective antibiotics: G418 (400 μg/ml) for Na$_v$1.5 or V5-His-tagged β-subunit cDNAs; Hygromycin (400 μg/ml) for V5-His-tagged β-subunit cDNAs transfected into cell lines stably expressing α-subunits; Zeocin (400 μg/ml) for wild-type or mutant β1B-subunit cDNAs in pTRACER-CMV2 or for the generation of the β1Fc cell line. Antibiotic-resistant colonies were isolated and characterized as described previously (Isom et al., 1995). To confirm stable transfection of pTRACER-CMV2 vectors, cells were plated in eight-chamber polystyrene vessel tissue culture-treated glass slides (Falcon; BD Biosciences Discovery Labware), rinsed with 1× PBS (Invitrogen), and fixed with 4% paraformaldehyde for 20 min at room temperature (RT). The slides were mounted on glass coverslips using Gel/Mount (Biomeda) and viewed using a Fluoview 500 confocal laser-scanning microscope (Olympus) with 100× objective. Images (1024 × 1024 pixels) were acquired with the Olympus Optical Fluoview software. To edit the figures for this study, images were exported to Adobe Photoshop CS3 Extended, version 10.0.1. Other than cropping, no other changes were made to the images.

Detection of β1V5 or β1BV5 by immunofluorescence. Cells expressing β1V5, β1Fc, β1BV5 alone, or hNav1.5 plus β1BV5 were used for immunofluorescent staining. Cells on glass coverslips or on eight-chamber slides were fixed briefly with 4% paraformaldehyde and washed 3 times
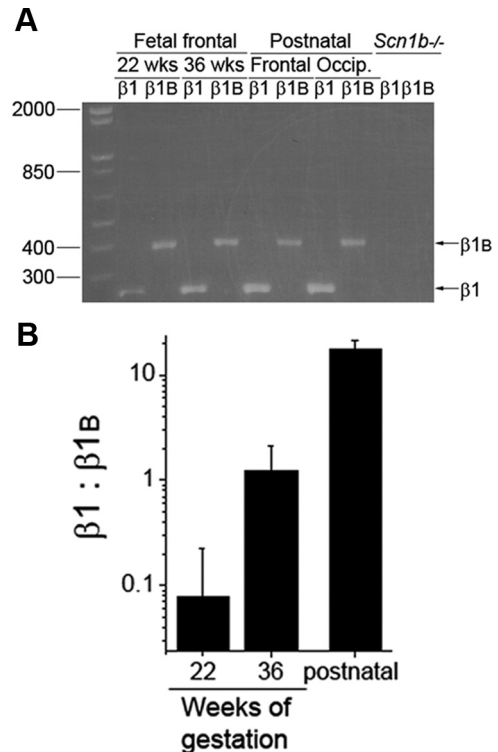

Figure 1. β1B is the predominant *SCN1B* splice variant during human fetal brain development. ***A***, Reverse transcriptase-PCR using primers for β1 or β1B performed with total RNA as template from human embryonic frontal lobe (22 week gestation, lanes 1 and 2; or 36 week gestation, lanes 3 and 4), postnatal frontal lobe (lanes 5 and 6), or postnatal occipital lobe (lanes 7 and 8). Samples of total RNA from *Scn1b*-null mouse brain were analyzed in parallel as negative controls (lanes 9 and 10). The gel shown is representative of triplicate experimental repeats. Nucleic acid markers are shown in base pairs. The arrows indicate β1 and β1B bands. ***B***, Quantitative PCR was performed with cDNAs generated from the RNA frontal lobe samples using the TaqMan assay as described in Materials and Methods. Ratios of β1 to β1B were compared using the $2^{-\Delta CT}$ method for each time point. Values are presented as mean ± SD. Note the logarithmic scale on the *y*-axis.

with 0.05 M phosphate buffer (PB) before use. Cells were permeabilized for a minimum of 1 h in PBTGS (0.1 M PB, 0.3% Triton X-100, and 10% normal goat serum) and incubated overnight with primary antibodies diluted in PBTGS. The following day, cells were incubated for 2 h in goat anti-mouse secondary antibody coupled to Alexa 594 (Invitrogen) diluted in PBTGS. Alternately, some cells were incubated with Alexa 488-conjugated anti-human IgG, Fcγ fragment antibody diluted in PBTGS for 2 h. Samples were washed three times with 0.1 M PB after each antibody step. Cells were incubated with DAPI for 20 min and washed again with 0.1 M PB. Samples were air-dried and mounted onto SuperFrost Plus slides using ProLong Gold antifade reagent with DAPI (Invitrogen). Digital images were collected using a Nikon A1R confocal microscope with Nikon NIS-Elements software located in the Department of Pharmacology, University of Michigan.

Western blot analysis. For each experiment, stably transfected cells from a 100 mm Petri dish, or transiently transfected cells from a 60 mm dish (at 95% confluence), were prepared for Western blot analysis as described previously (Patino et al., 2009). Western blot analysis was performed using the SNAP i.d. Protein Detection System (Millipore) according to the instructions of the manufacturer. All results presented are representative of at least three experimental repeats.

Surface biotinylation. Transfected cells were grown in four tissue culture plates (60 mm dishes for transiently transfected or 100 mm dishes for stably transfected cell lines) and membrane proteins biotinylated using the Cell Surface Labeling Accessory Pack (Thermo Fisher Scientific) following the manufacturer's instructions with Complete Mini (Roche) as protease inhibitor. Samples were loaded on a 10% SDS-PAGE gel and processed for Western blot. Immunoreactive signals were quantified using NIH ImageJ software and normalized to the level of Na^+/K^+ ATPase β1-subunit, a cell surface protein. All results presented are representative of at least three repeats.

Coimmunoprecipitation. Two hundred microliters of protein G-Sepharose 4B beads (Sigma-Aldrich) per sample of α plus β1 or α plus β1B cell lines were rinsed three times with 1× PBS and split into two microcentrifuge tubes. Beads were resuspended in 250 μl of dilution buffer (60 mm Tris-HCl, pH 7.5, 180 mm NaCl, 1.25% Triton X-100, 6 mm EDTA, pH 8, with Complete Mini Protease Inhibitor Tablets) and incubated overnight with end-over-end mixing at 4°C with 4 μg of mouse or rabbit pan-VGSC antibody or 4 μg of mouse or rabbit IgG, as indicated in the figure legends. Cells coexpressing α- plus β-subunits were resuspended in a 50 mm Tris, 10 mm EGTA, pH 8 solution (with Complete Mini) by scraping. The amount of sample used for each cell line was as follows: for HEKhNa$_v$1.1 cells transiently transfected or HEKhNa$_v$1.5 cells stably transfected with β1 or β1B, one 60 mm cell culture dish; for CHOhNa$_v$1.3 cells stably transfected with β1 or β1B, two 100 mm cell culture dishes. Cell suspensions were then centrifuged at 3000 × g for 10 min at 4°C. Cells were washed again in Tris/EGTA solution, resuspended in 1 ml of dilution buffer, and incubated 30 min on ice for lysis. After a centrifugation step to remove insoluble material, one-half of the supernatant was added to the beads incubated with anti-pan-VGSC antibody and the other one-half to the beads incubated with IgG. Beads with cell lysates were incubated with end-over-end mixing for 4 h at 4°C, and then washed three times with washing buffer (50 mm Tris, pH 7.5, 150 mm NaCl, 0.1% Triton X-100, 0.02% SDS, 5 mm EDTA, pH 8, with Complete Mini) and once with washing buffer without Triton X-100. Thirty-five microliters of Western blot sample buffer were then added to the beads, triturated, and incubated at 100°C for 5 min. Samples were then separated by SDS-PAGE on 10 or 18% polyacrylamide gels and transferred to nitrocellulose membranes for Western blot analysis.

Purification of β1B from conditioned media. Cells stably expressing V5-His epitope-tagged subunits were grown in one 850 cm² polystyrene
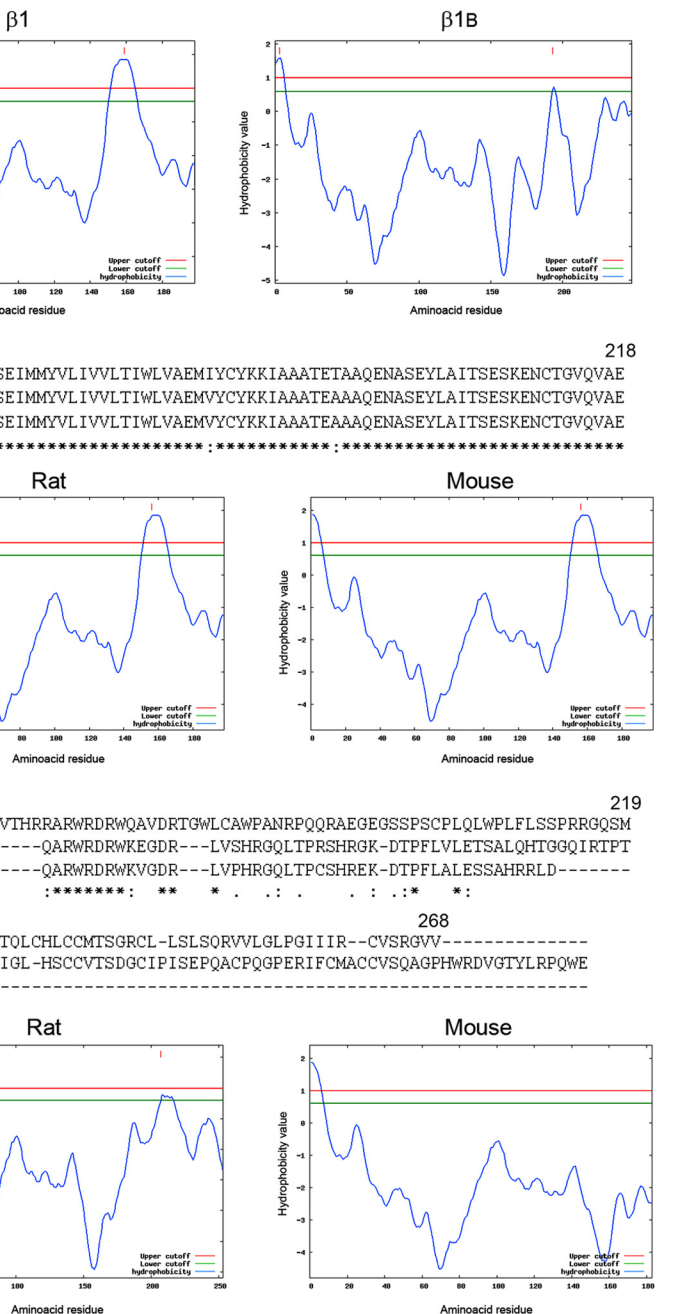

Figure 2. Hydrophobicity analysis of β1 and β1B. *A*, Hydrophobicity plots analyzing the amino acid sequences of human β1 (left panel) or β1B (right panel) show identical N-terminal signal peptides. β1, but not β1B, contains a transmembrane domain. *B*, The C-terminal region of β1 is conserved between species. Alignments of the predicted amino acid sequences of the C-terminal region of β1 encoded by exons 4 and 5 in human, rat, and mouse using the CLUSTALW algorithm. Numbers above all alignments correspond to the human sequence. *C*, Hydrophobicity plots analyzing the amino acid sequences of rat β1 (left panel) or mouse β1 (right panel) show predicted hydrophobic signal peptide and transmembrane domains. *D*, The unique C-terminal region of β1B is not conserved between species. Alignments of the predicted amino acid sequences of the unique C-terminal region of β1B encoded by retained intron 3 in human, rat, and mouse using the CLUSTALW algorithm. Numbers above all alignments correspond to the human sequence. *E*, Hydrophobicity plots analyzing the amino acid sequences of rat β1B (left panel) or mouse β1B (right panel) show hydrophobic signal peptides but no transmembrane domains.

roller bottle (Corning) containing 50 ml of media, or in 12 150 × 25 mm cell culture dishes (Corning) containing 20 ml of media per dish until confluent (8–15 d). The medium was not changed during this period but was supplemented with 1–2 ml of HI-FBS every 3–4 d. When cells reached confluence, conditioned media were collected and centrifuged to pellet cells that may have detached. The media were concentrated using a Millipore stirred cell concentrator, with a regenerated cellulose ultrafil-

tration membrane (nominal molecular weight limit, 10,000) (Millipore) to obtain a volume of ~50 ml. Complete EDTA-free Protease Inhibitor Cocktail (Roche) was added to prevent degradation. Concentrated conditioned media were mixed with 1.2 ml total volume of His-Select HF Nickel Affinity Gel (Sigma-Aldrich), previously rinsed with deionized water and equilibration/washing buffer (50 mM NaH₂PO₄, pH 8.0, 300 mM NaCl, 10 mM imidazole) in a Poly-Prep Chromatography Column (Bio-Rad), and incubated for 30 min at RT on a Clay Adams Nutator Mixer (BD Biosciences). The mix was then centrifuged at maximum speed in a swinging bucket rotor for 5 min. The supernatant was discarded, and the nickel gel was resuspended in 15 ml of equilibration/washing buffer. This washing step was repeated until the supernatant after centrifugation was completely clear. The nickel gel was resuspended in equilibration/washing buffer and transferred to the chromatography column in which the gel had been prerinsed. The nickel gel was then washed with 10 ml of equilibration/washing buffer, followed by elution buffer (50 mM NaH₂PO₄, pH 8.0, 300 mM NaCl, 250 mM imidazole), and the eluted fraction was collected in a Millipore Ultra-4 Centrifugal Filter Device with a 10,000 molecular weight cutoff regenerated cellulose filter (Millipore). The filter device was centrifuged at top speed in a swinging bucket rotor for 25 min, and the nonfiltered fraction was collected in a microcentrifuge tube where it was mixed with loading buffer containing SDS and β-mercaptoethanol at a 1:1 ratio. Western blot analysis was then performed. All results presented are representative of at least three repeats.

Cerebellar granule neuron neurite outgrowth assays. Neurite outgrowth assays from P14 mouse cerebellar granule neurons (CGNs) were described previously (Davis et al., 2004). Neurite length measurements were obtained from a minimum of 50 cells per condition from at least three independent experiments. Data from individual experiments were combined to provide an overall mean and SEM.

[³H]Saxitoxin binding. [³H]Saxitoxin ([³H]STX) binding was performed on intact cells, analyzed, and normalized to total cellular protein as previously described (McEwen et al., 2004).

Deglycosylation. Five microliters of whole-cell lysate from 1610-β1BV5 were treated with PGNase F (New England Biolabs; P0704S) following the instructions of the manufacturer. After enzymatic deglycosylation, the sample was mixed with Western blot sample buffer, separated by SDS-PAGE on a 10% polyacrylamide gel, and transferred to nitrocellulose for Western blot analysis. Another 5 μl aliquot of untreated whole-cell lysate was included on the Western blot as a negative control.

Whole-cell patch-clamp recording and analysis. Micropipettes were obtained from capillary glass tubing (Warner Instruments) using a horizontal P-97 puller (Sutter Instrument). Micropipettes resistance was between 1.5 and 3.5 MΩ, when filled with intracellular solution containing the following (in mM): 10 NaCl, 20 CsF, 95 CsCl, 10 EGTA, and 10 HEPES, pH 7.4 with CsOH; and the extracellular solution containing the following (in mM): 60 NaCl, 4 KCl, 1.5 CaCl₂, 1 MgCl₂, 5 glucose, 10 HEPES, 70 CsCl, pH 7.4 with NaOH. Voltage pulses were applied, and data were recorded using Clampex 9.2, Axopatch 200B amplifier, and a Digidata 1322A digitizer (Molecular Devices). Pipette and whole-cell capacitance were fully compensated. When appropriate, series resistance compensation was set to ~40–70% with the lag set to 10 μs. Signals were low-pass filtered at 5 kHz, and data were sampled at 40 kHz on-line. To determine the Na⁺ current amplitude and voltage dependence of activation, Na⁺ currents were evoked by depolarization to different 250 ms test pulses (from −110 to −70 mV at 10 mV intervals, from −70 to −10 mV at 5 mV intervals, and from −10 to 40 mV at 10 mV intervals) from a holding potential of −80 mV and a hyperpolarizing −120 mV, 500 ms prepulse. Peak Na⁺ current was normalized to cell capacitance and used to plot I–V curves and calculate conductance [$g = I/(V − V_{rev})$, where V is the test potential, and V_{rev} is the measured reversal potential]. Voltage dependence of inactivation was determined by applying a 50 ms test pulse of 0 mV after 250 ms prepulses to the same voltages as described for the voltage dependence of activation. Peak currents were normalized to the maximum peak I_{Na} amplitude. Normalized activation and inactivation curves were fit with a Boltzmann equation, $1/[1 + \exp(V − V_{1/2})/\kappa]$, where $V_{1/2}$ is the membrane potential in the midpoint of the curve, and κ is the slope factor. To assess the time course of recovery from inactiva-
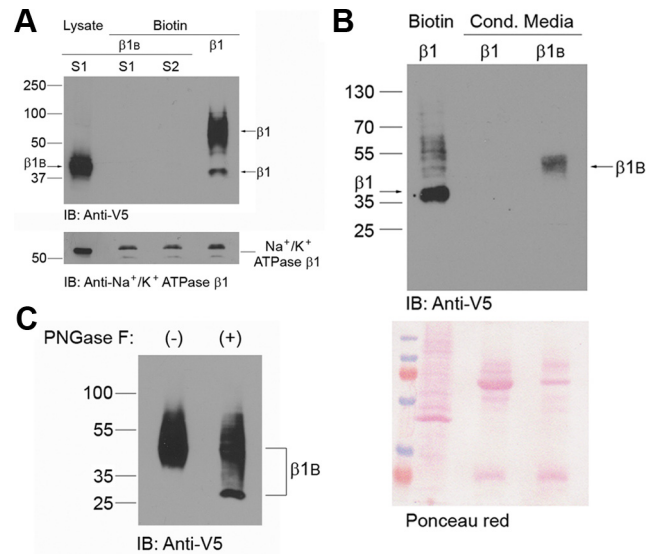

Figure 3. β1B is a secreted protein. *A,* β1 but not β1B is expressed at the cell surface. Western blot showing surface biotinylation of 1610 cells stably transfected with V5-His-tagged β1B (β1B) or V5-tagged β1 (β1) (top panel). Robust β1B expression was observed in the whole-cell lysate (Lysate S1). This same cell clone (S1) was assayed by surface biotinylation (Biotin S1), showing the absence of β1B at the cell surface. An independent β1B-V5 clone (S2) gave a similar result. A biotinylated sample from 1610 cells stably transfected with V5-His-tagged β1 (Biotin β1) was used as positive control for cell surface expression. A Western blot of the same samples with anti-Na⁺/K⁺ ATPase β1 showed equal loading of surface proteins (bottom panel). *B,* β1B but not β1 is expressed in conditioned media. Top panel, Conditioned media from 1610 cells stably expressing β1V5 (Cond. Media β1) or β1BV5 (Cond. Media β1B) were analyzed by Western blot and probed with anti-V5. A surface biotinylated sample of 1610-β1V5 cells (Biotin β1) is a positive control. Bottom panel, Ponceau red staining of the membrane demonstrates protein in all lanes. *C,* β1B is a glycoprotein. Western blot of 1610-β1BV5 whole-cell lysates before (left lane) and after (right lane) treatment with PNGase F. The bottom immunoreactive band is consistent with the molecular weight of fully deglycosylated β1B (~26 kDa). All blots are representative of three experimental repeats. Molecular weight markers are given in kilodaltons. The arrows indicate β1- or β1B-immunoreactive bands.

tion, a prepulse to 0 mV for 20 ms was followed by a recovery interpulse of variable duration (from 0.25 to 750 ms) to −120 mV and then a 25 ms test pulse to 0 mV to determine the fraction of recovered channels. Peak Na⁺ currents during the test pulse were normalized to the peak Na⁺ current during the corresponding prepulse and plotted as fractional recovery (F_r) against time. Data were then fit with one exponential to determine the time constants for recovery, using the equation $F_r = 1 − \exp((−x)/\tau)$, where τ is the constant of recovery. The kinetics of inactivation was measured on the test pulse to 0 mV from the same protocol used for voltage dependence of activation. The current, from 90% of the peak amplitude to 20 ms after the test pulse was initiated, was fitted to a double-exponential equation of the form $I = (F_f^* \exp(−t/\tau_f)) + (F_s^* \exp(−t/\tau_s) + C$, using the Chebyshev method, where I is the current, τ_f and τ_s are the time constants for the fast and slow inactivation component, and C is the steady-state persistent current. Analysis of the recorded Na⁺ current was performed using the software packages Clampfit 9.0.2 (Molecular Devices) and SigmaPlot 11.2 (Systat Software).

Clinical samples. A group of 360 unrelated probands [122 males (m) and 238 females (f)] diagnosed with epilepsy (n = 118; 42 m, 76 f), migraine (n = 110; 23 m, 87 f), Tourette's syndrome (n = 35; 23 m, 12 f), essential tremor (n = 25; 7 m, 18 f), bipolar disorder (n = 66; 24 m, 42 f), episodic ataxia (n = 4; 3 m, 1 f), episodic vertigo (n = 1 f), or episodic fainting (n = 1 f) were studied. Subjects were ascertained on the basis of family studies and routine clinical practice. Diagnoses were performed by clinicians specialized in these neurological disorders. For most patients, additional clinical information allowed for a better definition of the disease subphenotype, especially in cases of epilepsy, bipolar disorder, and migraine. The ethnic origin of all subjects is known, and additional affected and nonaffected family members for each proband

studied were collected for cosegregation/pedigree analysis. Informed consent was obtained from all participants, and study protocols were approved by the ethics committees of the institutions where collections occurred. An additional cohort of 192 unrelated Tourette's patient samples (150 m, 42 f) was used to assess involvement of the p.G257R variant in Tourette's syndrome.

Amplicon design and PCR for patient samples. Amplicons were designed to minimize the amount of intronic sequence and to avoid repetitive elements. PCR primers were designed using PrimerSelect (DNASTAR) and purchased from BioCorp. Primer sequences, amplicon sizes, and amplification conditions are given in Tables 1 and 2. Genomic DNA was isolated from blood samples using conventional methods. Samples were amplified using TaqDNA polymerase (QIAGEN) on a PE 9700 PCR thermocycler (PerkinElmer). Amplification conditions were determined by testing several annealing temperatures, and by addition of Q solution (QIAGEN) for problematic amplicons on control genomic DNA samples. All amplified fragments were tested by agarose gel electrophoresis.

Denaturing HPLC and sequence analysis. PCR fragments were optimized for melting temperature on a model 3500HT WAVE denaturing HPLC (dHPLC) (Transgenomic) with Wavemaker software, version 4.1.44. After PCR and dHPLC optimization, PCR fragments from DNA samples were amplified using the optimized conditions and the fragments were then tested on agarose gels. Amplified fragments were pooled four times, denatured at 95°C in a heating block for 5 min, and renatured slowly by cooling the block to 25°C over the course of 1 h. The pooled PCR fragments were run on the dHPLC apparatus at two different melting temperatures. The elution profiles of each sample pool were compared, and samples from one to three pools showing variant elution profiles were selected for sequence determination at the Genome Quebec Innovation Centre Sequencing Facility (Montréal, Québec, Canada). Sequencing reactions were performed on an ABI Prism 3700 sequencing apparatus using manufacturer's recommended conditions. Sequence traces were aligned using SeqManII (DNASTAR). Base pair variants were identified and annotated. Publicly available predicted single-nucleotide polymorphisms (SNPs) (from NCBI dbSNP, version 132) were identified, and those found in the sequence alignment were noted.

Genotyping of patient samples. Genotyping was performed by direct sequencing, allele-specific oligonucleotide (ASO) hybridization, or restriction fragment length polymorphism (RFLP) assay. Genotypes were scored manually or generated using Mutation Surveyor (SoftGenetics). For each ASO assay, two oligonucleotides were designed to differentiate wild-type from the mutant alleles. The ASO assays were done as described previously (Bourgeois and Labuda, 2004). Briefly, each oligonucleotide was end-labeled with [γ-^{32}P]dATP using T4 kinase in a 25 μl of total reaction volume. Probes were hybridized to nylon membranes to which was affixed the desired PCR amplified fragments, washed, and exposed to x-ray film. Films were scored and the genotypes for all successfully amplified samples were determined. The p.G257R variant was genotyped using an MspI RFLP assay. The 465 bp fragment from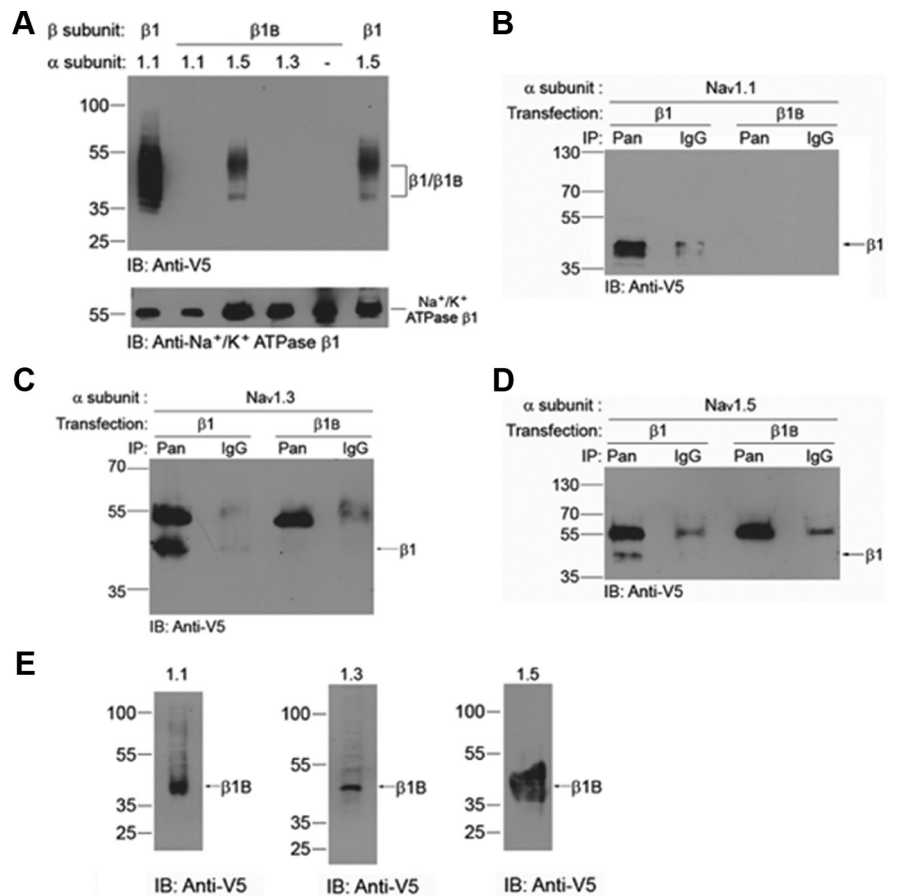 amplicon 3B (Table 1) was digested with MspI restriction enzyme (New England Biolabs), and the products were separated on a 1.5% agarose gel. The 257Gly allele yields digested products of 49, 87, 90, and 239 bp in size, whereas the 257Arg allele yields fragments of 49, 87, and 329 bp in size.

Statistical analyses. Continuous data, $n < 200$, were tested for normality using the Kolmogorov–Smirnov test. All continuous data were tested for homogeneity of variances using the Levene test. These data were normally distributed, and thus group means were compared using two-tailed Student's t test or ANOVA. If homogeneity of variance existed, Tukey's test was selected as the *post hoc* test; otherwise, Tamhane's T2 was used. Statistical significance was set at $p < 0.05$. SPSS was used for all determinations of statistical significance. The bar graphs were obtained using SPSS, Origin 7 (OriginLab Corporation), or Prism 5 (GraphPad).

Results

Expression patterns of β1 and β1B in human brain are developmentally regulated

We demonstrated previously that β1 and β1B mRNA have complementary expression patterns in rat brain (Kazen-Gillespie et

Figure 4. Cell surface expression and association of VGSC α- and β1- or β1B-subunits. **A**, β1B is located at the cell surface in the presence of Na$_v$1.5. Top panel, Cell surface biotinylation of cell lines stably expressing Na$_v$1.1, Na$_v$1.3, or Na$_v$1.5 cotransfected with β1BV5 (β1B-1.1, β1B-1.3, and β1B-1.5 lanes, respectively) analyzed by Western blot and probed with anti-V5. Surface biotinylation samples from cells coexpressing Na$_v$1.1 or Na$_v$1.5 with β1V5 (β1–1.1 and β1–1.5 lanes, respectively) were positive controls. Samples from cells coexpressing Na$_v$1.3 with β1V5 showed similar results (data not shown). A sample from 1610-β1BV5 cells, expressing no VGSC α-subunits (β1B "−" lane) served as a negative control. Bottom panel, Western blot of the same samples probed with anti-Na$^+$/K$^+$ ATPase β1 showed equal loading of surface proteins. Molecular weight (MW) markers are indicated in kilodaltons. Arrows, β1- or β1B-immunoreactive bands. **B–D**, Coimmunoprecipitation from Triton X-100-solubilized cells stably coexpressing Na$_v$1.1 (**B**), Na$_v$1.3 (**C**), or Na$_v$1.5 (**D**) with β1V5 or β1BV5, as indicated, was performed using anti-pan-VGSC antibody for immunoprecipitation (β1 Pan or β1B Pan) followed by anti-V5 to probe the Western blot. Immunoprecipitation with nonimmune IgG was performed as a negative control (β1 IgG or β1B IgG). **E**, Western blots of equal aliquots of whole-cell lysates of β1B-expressing cells used in **B–D** to confirm the presence of β1B: Na$_v$1.1 + β1B line (1.1, left panel), Na$_v$1.3 plus β1B line (1.3, middle panel), Na$_v$1.5 plus β1B line (1.5, right panel). All blots are representative of triplicate repeats. MW markers are given in kilodaltons. The arrows indicate immunoreactive β1 or β1B bands.
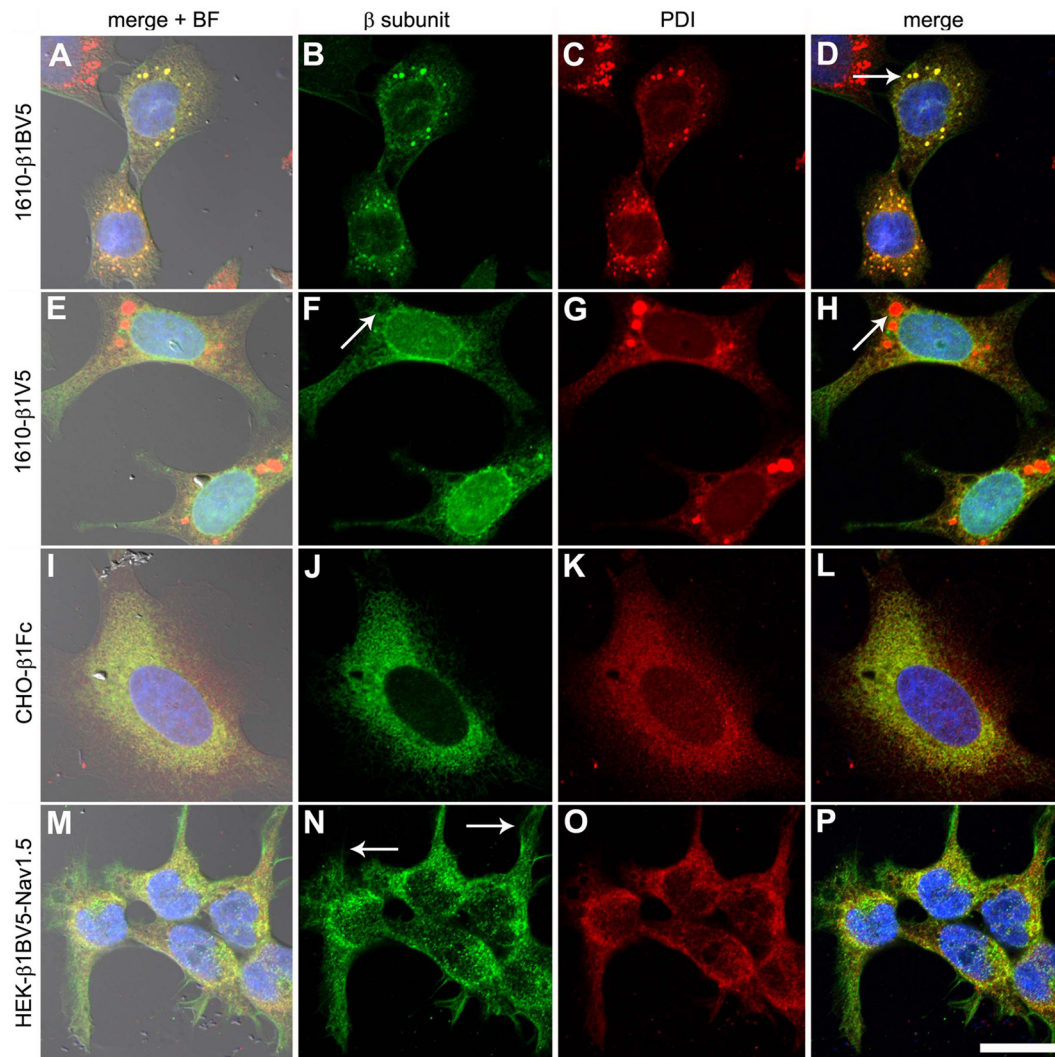
Figure 5. β1B is detected in the ER in the absence of Na$_v$1.5, and at the cell surface when coexpressed with Na$_v$1.5. Cells expressing β1V5, β1BV5, β1Fc, or β1BV5 plus Nav1.5 were labeled with anti-PDI to mark the ER, and anti-V5 or anti-Fc antibodies to label β-subunits. Merged images are presented with and without bright-field (BF) illumination to clearly show both fluorescent signal as well as identify cell borders. ***A–D***, 1610-β1BV5 cells display strong anti-V5 signal coincident with anti-PDI signal (***D***, arrow). ***E–H***, 1610-β1V5 cells display a diffuse anti-V5 signal but lack the ER localization seen in 1610-β1B cells, consistent with plasma membrane expression of β1 (***F***, ***H***, arrows). ***I–L***, CHO-β1Fc cells display strong overlap of anti-Fc and anti-PDI immunofluorescence, consistent with the nature of β1Fc as a secreted protein. ***M–P***, HEK-β1BV5-Nav1.5 cells display diffuse anti-V5 signal that extends beyond the ER, including expression within filipodial structures at the cell border (***N***, arrows). Scale bar, 20 μm.

al., 2000). β1B is expressed predominantly during embryonic rat brain development, with levels decreasing after birth. In contrast, β1 expression is low in embryonic rat brain, but becomes dominant over β1B in postnatal brain. To determine whether this developmental expression pattern is conserved in humans, we performed RT-PCR using primers specific for β1 or β1B and human frontal lobe total RNA as template. Samples were obtained from both human embryonic brain (22 and 36 weeks of gestation) and human postnatal brain (age range, 9–56 years). In addition, we obtained occipital lobe total RNA from the postnatal subjects. RNA from *Scn1b*-null mouse brain was used as a negative control. At the earliest time point assayed, 22 weeks of gestation, both variants were detected, although higher levels of β1B were detected compared with β1. As development progressed, the level of β1B appeared to remain relatively constant while the level of β1 increased (Fig. 1*A*). To quantify these results, we prepared cDNA from each RNA sample and performed quantitative PCR using the TaqMan assay. Ratios of β1 to β1B were compared using the $2^{-\Delta CT}$ method. At 22 weeks of gestation,

β1:β1B = 0.08 (mean $2^{-\Delta CT}$ ± SD, 0.08 ± 0.15). At 36 weeks of gestation, β1B and β1 levels were similar (β1:β1B, 1.22 ± 0.91). After birth, levels of β1 transcript were ~18-fold higher than β1B (β1:β1B, 17.84 ± 3.45; Fig. 1*B*). We found no significant differences between results obtained from the various postnatal subjects (data not shown), and thus these values were pooled.

VGSC β1B is a secreted protein

The topology of β1 is well understood (Isom et al., 1992); however, less is known about β1B. *In silico* analyses of the predicted amino acid sequences of human β1 and β1B were performed using the Goldman Engelman Steitz hydrophobicity scale as described in Materials and Methods. In contrast to β1 (Isom et al., 1992), a hydrophobic transmembrane domain was not predicted for β1B (Fig. 2*A*). The predicted β1 and β1B amino acid sequences from rat and mouse were analyzed similarly for hydrophobicity. In contrast to predicted amino acid sequences for β1 from these species, which are highly conserved and contain predicted hydrophobic domains (Fig. 2*B*,*C*), very little similarity

was found in the C-terminal region unique to β1B, suggesting that the sequence of this domain is species specific (Fig. 2D). Importantly, none of these unique β1B sequences contained a predicted transmembrane domain, suggesting that β1B may be a secreted protein (Fig. 2E).

To investigate whether β1B is indeed a secreted protein, we stably transfected Chinese hamster lung 1610 fibroblasts with a V5-His epitope-tagged human β1B cDNA construct (1610-β1BV5). Protein expression at the cell surface was assessed by surface biotinylation, probing the final Western blot with anti-V5 antibody. 1610 cells stably expressing β1V5 (1610-β1V5) were used as a positive control (Patino et al., 2009), and as expected, β1V5 was detected at the cell surface (Fig. 3A). In contrast, β1BV5 was not detected at the cell surface despite abundant levels of β1BV5 protein in the whole-cell lysate sample (Fig. 3A). We next assayed conditioned media by Western blot to test for the presence of β1B. Anti-V5-immunoreactive bands were present in conditioned media from 1610-β1BV5 cells, while, as expected, no bands were detected in media from 1610-β1V5 cells despite high levels of protein present on the Ponceau red-stained blot (Fig. 3B).

The migration of β1B by SDS-PAGE was variable, over a size range of $\sim$26 kDa (the predicted molecular weight of nonglycosylated β1B) to 45 kDa, with the majority of experimental results showing the $\sim$45 kDa band. Interestingly, the same clonal line of 1610-β1BV5 cells yielded bands of different sizes in different experiments. We hypothesized that these bands might represent different glycosylation states of β1B and that enzymes present in the culture medium or experimental solutions might result in artifactual deglycosylation of this protein. To test this, whole-cell lysates of 1610-β1BV5 cells were treated with PNGase F and samples were then analyzed by Western blot. PNGase F treatment resulted in collapse of the β1B-immunoreactive band from $\sim$45 to $\sim$26 kDa (Fig. 3C), suggesting that the various immunoreactive β1B bands identified in the conditioned media represent different glycosylation states. Together, these data suggest that both β1 and β1B are glycoproteins. Furthermore, they suggest that, while β1 has transmembrane topology, β1B is a secreted protein that may be critical during embryonic brain development.

Differential effects of VGSC α-subunits on β1B cell surface expression

The experiments in Figure 3 demonstrate that β1B is secreted from cells that do not express VGSCs. To test whether the presence of a VGSC α-subunit may result in retention of β1B at the cell surface, we studied cell lines coexpressing human β1BV5 with human VGSC α-subunits. Because *SCN1B* mutations affecting the region specific to β1B are associated with cardiac arrhythmia (Watanabe et al., 2008) and epilepsy (shown here), we tested the effects of human Na$_v$1.1, a common target of genetically determined epilepsy (Meisler et al., 2010), and human Na$_v$1.5, the

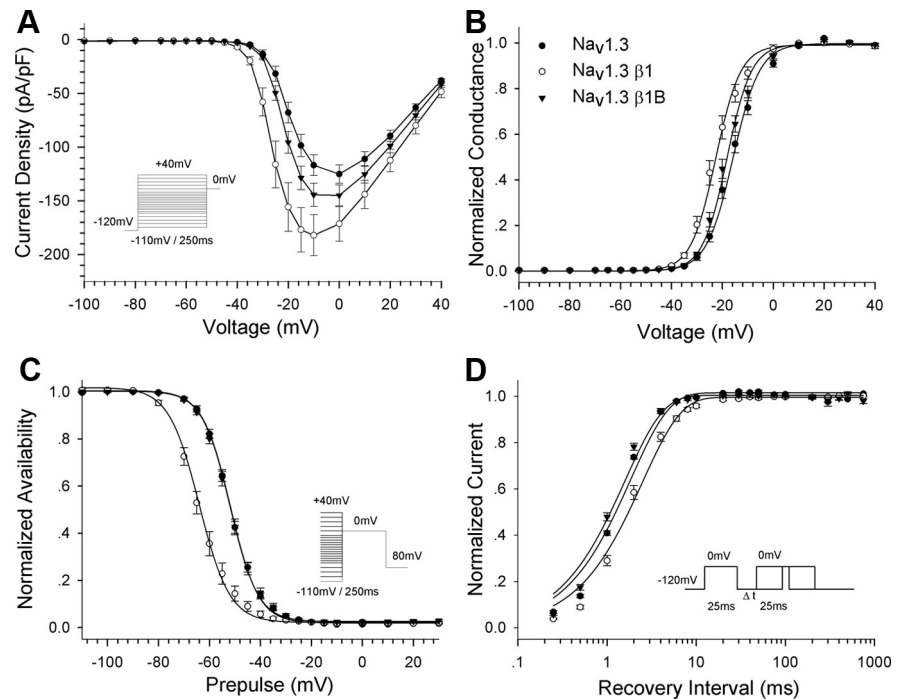**Figure 6.** β1B has subtle effects on Na$_v$1.3-generated Na$^+$ current. CHOhNa$_v$1.3 (closed circles), CHOhNa$_v$1.3β1 (open circles), or CHOhNa$_v$1.3β1B (closed triangles) cells were tested using the whole-cell patch-clamp technique as described in Materials and Methods. **A**, Current density: Na$^+$ current density is increased in the presence of β1 but not by β1B. **B**, Voltage dependence of activation: β1 coexpression results in negative shifts in the voltage dependence of activation. Coexpression of β1B was not different from Na$_v$1.3 alone. **C**, Voltage dependence of inactivation: β1 coexpression results in negative shifts in the voltage dependence of inactivation. Coexpression of β1B was not different from Na$_v$1.3 alone. **D**, Recovery from inactivation: Coexpression of β1 increased while β1B decreased τ. The insets in **A**, **C**, and **D** represent voltage protocols. **A** and **B** were obtained using the same protocol. Data points represent mean $\pm$ SEM. The solid lines represent the mean of every individual fit. Biophysical properties are provided in Table 3.

VGSC α-subunit most prevalent in heart and a target of inherited arrhythmia (Catterall et al., 2005; Remme et al., 2008; Ruan et al., 2009). In addition, because β1B is mainly expressed during embryonic brain development (Fig. 1), we tested the effects of human Na$_v$1.3, the predominant VGSC expressed in embryonic brain (Catterall et al., 2005). For unknown reasons, we were unable to establish stable β1V5- or β1BV5-expressing cell lines using HEKhNa$_v$1.1 cells (Patino et al., 2009). Thus, all experiments with this cell line were performed following transient transfection of β1V5 or β1BV5 cDNA. We were able to establish stable β-subunit-expressing lines using HEK cells stably transfected with human Na$_v$1.5 (HEKhNa$_v$1.5). Finally, Chinese hamster ovary fibroblasts stably expressing human Na$_v$1.3 (CHOhNa$_v$1.3) (Meadows et al., 2002a) were stably transfected with human β1 or β1B cDNAs. Similar to 1610 cells expressing no VGSC α-subunits, β1B was not detected at the surface of cells coexpressing Na$_v$1.1 or Na$_v$1.3 (Fig. 4A), suggesting that β1B is secreted despite the presence of these channels. In contrast, cell surface β1B expression was detected in biotinylated samples from cells coexpressing Na$_v$1.5 and β1B (Fig. 4A), suggesting that β1B may be selectively retained at the cell surface by this channel and consistent with previous results showing modulation of Na$_v$1.5-mediated Na$^+$ current by β1B (Watanabe et al., 2008).

Effects of β1 and β1B on VGSC α-subunit cell surface expression

β1 associates with multiple VGSC α-subunits and increases their functional expression. For example, β1 associates with Na$_v$1.2 and this association is functionally detected by increased Na$^+$

current density and by increased cell surface [^{3}H]STX binding (Isom et al., 1995; McEwen et al., 2004). Rat β1B increases the cell surface expression of rat Na$_v$1.2 in transfected cells, with subtle changes in current activation and inactivation, suggesting that these subunits functionally associate (Kazen-Gillespie et al., 2000). Similarly, human β1B coexpression increases Na$^+$ current density generated by human Na$_v$1.5 (Watanabe et al., 2008), again suggesting functional association. In the following set of experiments, we asked whether specific α- and β1- or β1B-subunits associate and whether coexpression of β1 or β1B results in increased α-subunit cell surface expression.

We used coimmunoprecipitation assays to examine whether human β1B associates with human Na$_v$1.1, human Na$_v$1.3, or human Na$_v$1.5. In these experiments, anti-pan-VGSC antibody was used for the immunoprecipitation step from Triton X-100-solubilized whole-cell lysates, and Western blots were probed with anti-V5 to detect associated β-subunits. β1 coprecipitated with Na$_v$1.1 (Fig. 4*B*), Na$_v$1.3 (Fig. 4*C*), and Na$_v$1.5 (Fig. 4*D*). In contrast, β1B association was not detected with any α-subunit (Fig. 4*B–D*). Western blots of whole-cell lysates from each cell line coexpressing α- and β1BV5-subunits demonstrated the presence of β1B in all three (Fig. 4*E*). Lack of association between Na$_v$1.5 and β1B in the coimmunoprecipitation assay contrasts with our result above, showing cell surface retention of β1B in the presence of Na$_v$1.5, and with those of others (Watanabe et al., 2009). Possible explanations for this discrepancy may be that the interaction between β1B and Na$_v$1.5 is disrupted by detergent solubilization or that Na$_v$1.5 and β1B associate transiently or with low affinity such that their interaction cannot be captured biochemically.

We performed immunofluorescent labeling of cells transfected with β1BV5, β1V5, β1Fc, or β1BV5 plus Na$_v$1.5 to assess the subcellular localization of each of these β-subunits (Fig. 5). Anti-V5 staining of β1BV5 cells demonstrates β1B ER localization, as indicated by anti-V5 immune signal coincident with that for the ER marker PDI (Fig. 5*A–D*). In contrast, β1V5, which has been shown previously to be a transmembrane protein (Isom et al., 1992), is more evenly distributed in all cell areas, including the cell surface (Fig. 5*E–H*). As a control for the subcellular distribution of a known secreted protein, we performed a similar labeling experiment using β1Fc, which we have shown previously to be a secreted protein (McEwen and Isom, 2004) (Fig. 5*I–L*). This engineered, secreted form of β1 displays strong overlapping fluorescent signals with that of PDI, similar to the overlap observed in β1BV5 cells. Finally, we stained cells coexpressing β1BV5 plus Na$_v$1.5 subunits with anti-V5 and anti-PDI to visualize β1B in the presence of a VGSC α-subunit (Fig. 5*M–P*). In addition to its localization in intracellular organelles, and consistent with surface biotinylation assays (Fig. 4*A*), β1BV5 staining was detectable at the cell surface (Fig. 5*N*, arrows), particularly in filopodia-like extensions at the cell borders. Together, these immunofluorescence results suggest that β1B is a secreted protein. Furthermore, they confirm that the subcellular distribution of β1B is altered when coexpressed with Na$_v$1.5.

[^{3}H]STX binding to intact cells was used to assay Na$_v$1.3 cell surface expression in the presence and absence of β-subunits. Because STX is membrane impermeant, binding to intact cells measures only cell surface and not intracellular channels (McEwen et al., 2004, 2009). As expected, β1 significantly increased cell surface [^{3}H]STX binding compared with Na$_v$1.3 alone (Na$_v$1.3 plus β1, 8.93 ± 0.72 fmol/mg, vs Na$_v$1.3 alone, 5.53 ± 0.65 fmol/mg; $n = 9$ for each subunit combination; $p < 0.001$). In contrast, β1B did not significantly increase cell surface [^{3}H]STX binding com-

Table 3. Electrophysiological analysis of Na$^+$ currents

	Na$_v$1.3	Na$_v$1.3 β1	Na$_v$1.3 β1B
Voltage dependence of activation			
$V_{1/2}$ (mV)	−15.76 ± 0.98	−22.59 ± 1.22*	−18.15 ± 0.91
k	5.21 ± 0.21	4.88 ± 0.26	4.80 ± 0.84
n	21	15	23
Voltage dependence of inactivation			
$V_{1/2}$ (mV)	−51.77 ± 0.63	−63.97 ± 1.40*	−51.92 ± 0.85
k	−5.47 ± 0.13	−5.96 ± 0.31	−5.43 ± 0.17
C	0.02 ± 0.001	0.02 ± 0.002	0.02 ± 0.003
n	21	15	23
Kinetics of inactivation			
τ_{slow} (ms)	4.00 ± 0.31	3.58 ± 0.31	3.92 ± 0.32
Amplitude$_{slow}$ (%)	12.27 ± 0.87	8.96 ± 0.95**	9.51 ± 0.68**
τ_{fast} (ms)	0.65 ± 0.03	0.49 ± 0.04***	0.56 ± 0.02***
Amplitude$_{fast}$ (%)	76.41 ± 0.91	78.47 ± 0.88	79.14 ± 0.99
C	3.30 ± 0.25	2.42 ± 0.47	3.14 ± 0.46
n	20	14	20
Kinetics of recovery			
τ (ms)	1.86 ± 0.04	2.61 ± 0.16*	1.63 ± 0.06*
n	17	12	22

Data are mean ± SEM.

*$p < 0.001$ versus Na$_v$1.3 alone; **$p < 0.05$ versus Na$_v$1.3 alone; ***$p < 0.01$ versus Na$_v$1.3 alone.
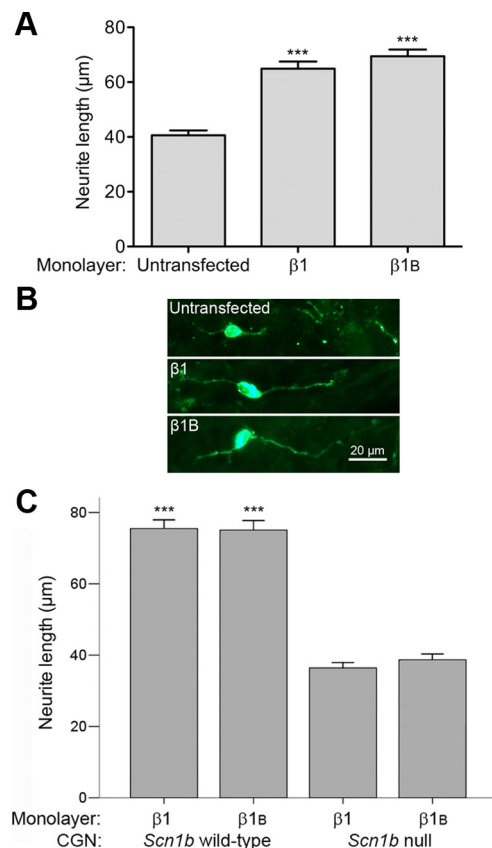

Figure 7. β1B stimulates neurite outgrowth of CGNs. ***A***, Neurite lengths of CGNs isolated from wild-type mice grown on 1610 cells (Untransfected) or 1610 cells stably expressing β1V5 (β1) or β1BV5 (β1B) measured as described in Materials and Methods. Significance, ***$p < 0.001$. ***B***, Examples of increased neurite length. CGNs grown on CHL monolayers were fixed in 4% paraformaldehyde for 10 min and then processed for immunocytochemistry using an anti-GAP43 antibody (1:500; Millipore), as described previously (Davis et al., 2004). ***C***, Neurite lengths of CGNs from wild-type and *Scn1b*-null mice grown on 1610 cells stably expressing β1V5 or β1BV5. Significance, ***$p < 0.001$. All data are presented as mean ± SEM.

pared with cells expressing only Na$_v$1.3 (Na$_v$1.3 plus β1B, 5.90 ± 0.92 fmol/mg).

Functional modulation of Na$^+$ current by β1B

We showed previously that rat β1B exerted subtle but significant effects on rat Na$_v$1.2-generated Na$^+$ current activation and inactivation in transfected cells (Kazen-Gillespie et al., 2000). To examine whether coexpression of β1 or β1B modulated Na$_v$1.3-generated Na$^+$ current, we performed whole-cell patch-clamp recordings on CHO hNa$_v$1.3 cells in the presence and absence of stable expression of human β1 or β1B. Consistent with our coimmunoprecipitation and [^{3}H]STX binding results, β1 coexpression had significant effects on Na$^+$ current. β1 significantly increased Na$^+$ current density at test potentials over a range from −45 to 0 mV (Fig. 6A) and shifted the voltage dependence of activation by ~6 mV and the voltage dependence of inactivation by ~12 mV, both in the hyperpolarizing direction. In contrast, β1B produced more subtle changes. β1B coexpression resulted in a minor increase in Na$^+$ current density and a small hyperpolarizing shift in the voltage dependence of current activa-

tion; however, these changes were not statistically significant (Fig. 6A,B). β1B had no measurable effect on the voltage dependence of current inactivation (Fig. 6C). Both β1 and β1B modulated the kinetics of inactivation and recovery from inactivation (Fig. 6D, Table 3). β1 and β1B decreased the time constant, τ, of fast inactivation, although β1 had a more significant effect than β1B (Table 3). Interestingly, β1 and β1B had opposite effects on the kinetics of recovery from inactivation: β1 coexpression increased, while β1B expression decreased, τ compared with α alone. In summary, coexpression of Na$_v$1.3 plus β1 resulted in increased Na$^+$ current density, decreased channel availability, acceleration of the development of fast inactivation, and deceleration of the rate of recovery from inactivation compared with Na$_v$1.3 alone. In contrast, coexpression of Na$_v$1.3 plus β1B accelerated the development of fast inactivation and increased the rate of recovery from inactivation compared with Na$_v$1.3 alone. These results suggest that, even though secreted, β1B may exert subtle effects on Na$^+$ current in brain neurons. Furthermore, these effects may be autocrine or paracrine.

β1B stimulates neurite outgrowth in CGNs through β1 adhesion

VGSC β-subunits contain a single extracellular Ig domain and function as CAMs (Malhotra et al., 2000, 2002; McEwen and Isom, 2004). β1 promotes CGN neurite outgrowth *in vitro* and *in vivo* through *trans* homophilic cell-adhesive interactions (Davis et al., 2004; Brackenbury et al., 2008a, 2010). Because β1 and β1B contain identical Ig loop domains, we hypothesized that β1B may function as a secreted CAM to promote neurite outgrowth. Previous results using an engineered soluble β1 extracellular domain to promote CGN neurite outgrowth and to bind to other CAMs support this idea (Davis et al., 2004; McEwen and Isom, 2004). To test this hypothesis, we investigated the ability of β1B to promote
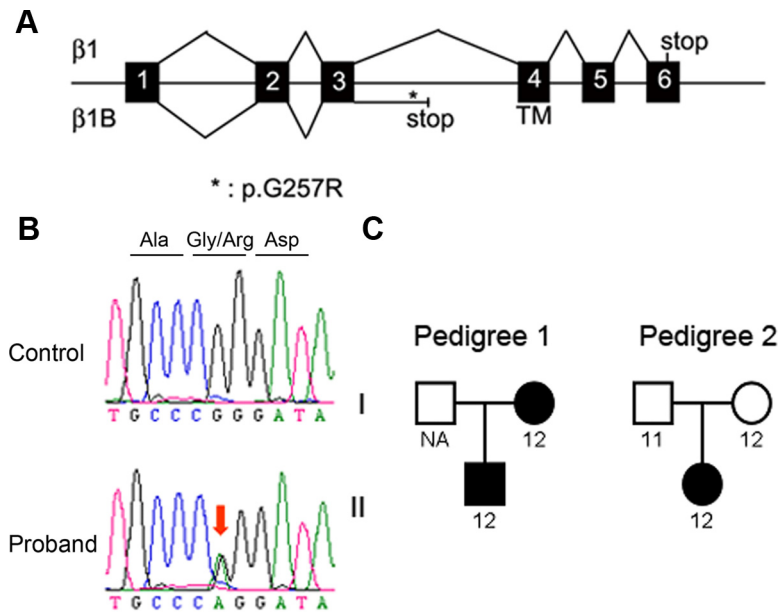

Figure 8. A *SCN1B* mutation that affects β1B is found in two pedigrees of idiopathic epilepsy. ***A***, Genomic structure of *SCN1B*. Exons 1– 6 constitute β1. Extension of exon 3 into intron 3 generates the variant, β1B. The novel 3′ end of β1B does not contain a transmembrane domain (TM). The asterisk (*) indicates the position of the G257R mutation. (This is not drawn to scale.) ***B***, Chromatogram showing the p.G257R heterozygous missense mutation in the epilepsy proband from pedigree 1 (bottom row), whereas it is absent from a control individual (top row). ***C***, Two pedigrees segregating the p.G257R missense mutation. Pedigree 1 has epilepsy, whereas pedigree 2 has epilepsy and Tourette's syndrome. Affected individuals are indicated with black symbols, and normal individuals are shown with white symbols. 1, 257Gly allele; 2, 257Arg allele. NA, Not available.

neurite outgrowth of CGNs. CGNs were isolated from P14 C57BL/6 mice and plated on monolayers of untransfected 1610 cells (as a negative control), 1610-β1V5 cells (as a positive control), or 1610-β1BV5 cells, as described in Materials and Methods. After 24 h of incubation, cells were fixed and immunostained with anti-GAP43, and the length of the longest neurite was measured. Consistent with previous results (Davis et al., 2004; Brackenbury et al., 2008a), the mean neurite length of CGNs plated on 1610-β1V5 cells (mean ± SE, 64.88 ± 2.63 μm) was significantly greater than CGNs plated on 1610 cells (40.64 ± 1.70 μm). Importantly, the mean neurite length of CGNs plated on 1610-β1BV5 cells (69.43 ± 2.46 μm) was also statistically greater than CGNs plated on 1610 cells, and not significantly different from cells plated on 1610-β1V5 cells (n = 300 for each group; p < 0.001; Fig. 7A). Examples of CGN neurite length are shown in Figure 7B. Thus, similar to β1, β1B functions as a CAM to promote neurite outgrowth. In contrast to β1, however, we propose that β1B functions as a secreted rather than as a transmembrane CAM.

The neurite outgrowth-promoting activity of β1 is abolished in CGNs isolated from *Scn1b*-null mice (Davis et al., 2004), demonstrating that *trans* homophilic β1–β1 interactions are required. To test whether a similar requirement of β1 expression on the neuron exists for β1B signaling, we compared neurite outgrowth of CGNs isolated from *Scn1b*-null mice versus wild-type controls plated on β1B-secreting monolayers. In agreement with our previous studies (Davis et al., 2004), the mean neurite length of wild-type CGNs plated on 1610-β1V5 cells (75.46 ± 2.44 μm) was statistically greater than for *Scn1b*-null CGNs (36.42 ± 1.45 μm). Similarly, the mean neurite length of wild-type CGNs plated on 1610-β1BV5 cells (75.06 ± 2.71 μm) was significantly higher than that of null CGNs (38.66 ± 1.69 μm; n = 300 per condition; p < 0.001; Fig. 7C). There was no significant differ-

Table 4. Identified human SCN1B variants

| | | | | | | | Allelic frequencies by cohort[a] | | | | | | | | | | |
| | | | | | | | Epilepsy | | Migraine | | Bipolar | | Tourette | | ET | | |
Exon	Position	dbSNP	Allele 1	Allele 2	Impact	MAF	1	2	1	2	1	2	1	2	1	2	Total
1	chr19:40213619	None	G	T	g. +15 after the end of exon 1	nd	nd	nd	nd	nd	nd	nd	nd	nd	nd	nd	nd
3	chr19:40216664	rs55742440	T	C	Leu210Pro	0.394	136	94	132	86	83	45	38	32	30	20	696
3	chr19:40216676	None	G	A	Arg214Gln	0.005	227	1	219	1	122	2	69	1	50	0	692
3	chr19:40216779	None	C	A	Ser248Arg	0.147	197	33	184	34	109	19	54	16	47	3	696
3	chr19:40216784	None	G	C	Arg250Thr	0.149	198	34	185	33	108	20	54	16	46	4	698
3	chr19:40216804	None	G	A	Gly257Arg	0.002	231	1	220	0	128	0	69	1	50	0	700
5	chr19:40222354	rs28365107	T	G	g. −25 before the start of x05	nd	nd	nd	nd	nd	nd	nd	nd	nd	nd	nd	nd
5	chr19:40222365	rs28365109	C	A	g. −14 before the start of x05	nd	nd	nd	nd	nd	nd	nd	nd	nd	nd	nd	nd
5	chr19:40222457	rs28365106	C	T	g. +6 after the end of x05	nd	nd	nd	nd	nd	nd	nd	nd	nd	nd	nd	nd
5	chr19:40222507	None	G	T	g. +59 after the end of x05	nd	nd	nd	nd	nd	nd	nd	nd	nd	nd	nd	nd
6	chr19:40222530	rs28365105	C	G	g. −18 before the start of x06	nd	nd	nd	nd	nd	nd	nd	nd	nd	nd	nd	nd
6	chr19:40222577	rs2278995	T	C	3′-UTR + 42 after the stop codon	0.135	197	31	179	33	106	20	54	14	47	3	684
6	chr19:40222621	rs2278996	A	C	3′-UTR + 86 after the stop codon	nd	nd	nd	nd	nd	nd	nd	nd	nd	nd	nd	nd
6	chr19:40222718	None	C	A	3′-UTR + 184 after the stop codon	nd	nd	nd	nd	nd	nd	nd	nd	nd	nd	nd	nd

ET, Essential tremor; nd, not done.

[a]Number of chromosomes from each disease cohort with either allele 1 or 2.

ence between the mean neurite lengths of wild-type or null CGNs plated on 1610-β1V5 cells versus those on 1610-β1BV5 cells. These data demonstrate that the neurite outgrowth-promoting ability of β1B requires interaction with β1-subunits present at the neuronal surface, similar to the mechanism described for β1 (Brackenbury et al., 2008a, 2010).

A SCN1B mutation affecting β1B may be a risk factor for idiopathic epilepsy

Mutations in SCN1B are associated with human disease, including epilepsy and cardiac arrhythmia (Scheffer et al., 2007; Watanabe et al., 2008, 2009; Patino et al., 2009). While one mutation specific to the region encoding β1B is linked to Brugada syndrome (Watanabe et al., 2008), to date all of the SCN1B epilepsy mutations occur in the Ig domain shared by β1 and β1B (Patino and Isom, 2010). To test the hypothesis that SCN1B mutations specifically affecting β1B and not β1 may be associated with epilepsy as well as arrhythmia, all SCN1B exons and intron 3, which is retained in β1B (Fig. 8A) (Kazen-Gillespie et al., 2000; Qin et al., 2003), were amplified by PCR as part of a screening study of 150 genes in 360 unrelated patients with episodic brain disorders (118 with epilepsy, 110 with migraine, 66 with bipolar disorder, 35 with Tourette's syndrome, 25 with essential tremor, 4 with episodic ataxia, 1 with episodic vertigo, and 1 with episodic syncope). A total of 14 SCN1B variants were identified, of which 5 resulted in amino acid substitutions in the unique region encoding β1B (Table 4). Of these, three had minor allele frequencies (MAFs) > 0.1 (p.L210P, p.S248R, and p.R250T) and occurred in all cohorts of patients. A variant (p.R214Q) had MAF = 0.005 but was also present in four of eight cohorts. One variant (p.G257R) was identified in two unrelated probands with idiopathic epilepsy (MAF = 0.002) as a heterozygous mutation (Fig. 8B). One of those probands belonged originally to the Tourette's cohort, but

upon further clinical investigation this patient was found to be comorbid for epileptic seizures, suggesting that this variant was associated with an epilepsy phenotype. The patient from pedigree 1 had tonic-clonic seizures starting from 10 years of age. The proband's mother and maternal aunt also had a history of seizures. The patient from pedigree 2 had right temporal seizures with secondary generalized seizures starting at 15 years of age, sometimes preceded by an aura. Seizures were controlled by Tegretol. This patient was also diagnosed with Gilles de la Tourette syndrome, with facial tics and aggressive impulsions. There was no family history of epilepsy in either parent.

To further examine whether the p.G257R variant was associated with Tourette's syndrome, an additional 192 unrelated Tourette's probands were genotyped (data not shown). The variant was not detected in this additional cohort, suggesting that p.G257R is not associated with increased risk of Tourette's syndrome. We screened an additional 187 normal control samples for the portion of intron 3 encoding the unique region of the β1B splice variant. One normal individual was identified with the p.G257R variant, perhaps suggesting incomplete penetrance similar to other SCN1B mutations (Scheffer et al., 2007; Watanabe et al., 2008).

To examine the segregation of p.G257R, additional samples from the probands' available family members were genotyped. For pedigree 1, both the proband and her mother carried the mutation and suffered from epilepsy. For pedigree 2, the mutation was inherited from the mother, but there was no reported history of seizures in either parent (Fig. 8C).

β1B p.G257R is a trafficking-deficient mutation resulting in a functional null allele

To investigate the mechanism by which β1B p.G257R might contribute to seizures, we stably transfected 1610 cells with V5-His-tagged p.G257R cDNA (1610-p.G257RV5). In contrast to wild-type
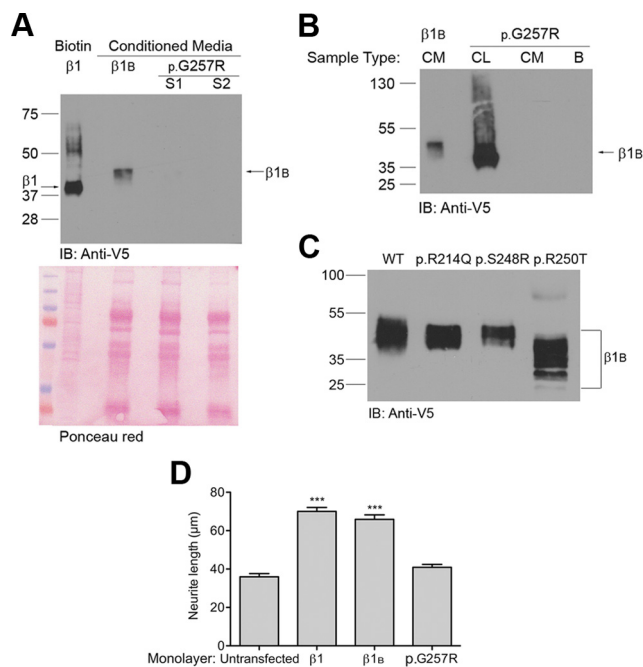
Figure 9. β1B p.G257R is a trafficking-deficient mutant. *A*, β1B but not p.G257R is detected in conditioned media. Top panel, Conditioned media from 1610 cells stably expressing β1BV5 (Cond. Media β1B) or p.G257RV5 (Cond. Media p.G257R S1 and S2, 2 independent cell clones) were collected, analyzed by Western blot, and probed with anti-V5. A surface biotinylated sample from the 1610-β1V5 clone (Biotin β1) was used as a positive control. Bottom panel, Ponceau red staining of the nitrocellulose shows protein in all lanes. *B*, p.G257R is retained intracellularly. Western blot analysis of whole-cell lysate (p.G257R CL), surface biotinylated cells (p.G257R B), or conditioned media (p.G257R CM) from the same 1610-p.G257RV5 cell clone. Conditioned media from 1610-β1BV5 cells (β1B CM) shows normal secretion of β1B. *C*, β1B polymorphic variants p.R214Q, p.S248R, and p.R250T are secreted into conditioned media similar to wild-type β1B, as indicated. *D*, p.G257R does not stimulate neurite outgrowth. Neurite lengths of CGNs isolated from wild-type mice grown on 1610 cells (Untransfected), 1610 cells stably expressing β1V5 (β1), 1610 cells stably expressing β1BV5 (β1B), or 1610 cells stably expressing p.G257RV5. Data are mean ± SE. Significance, ***$p < 0.001$. All Western blots are representative of three repeats. Molecular weight markers are given in kilodaltons.

β1BV5, p.G257RV5 was not detected in conditioned media (Fig. 9*A*) despite high levels of expression of the protein in the whole-cell lysates (Fig. 9*B*) and overall protein expression in the Ponceau red-stained blot (Fig. 9*A*, bottom panel). We used surface biotinylation assays to determine whether p.G257RV5 might be present at the cell surface. As demonstrated in Figure 9*B*, p.G257RV5 was detected in the whole-cell lysate but not in the conditioned media or on the cell surface. From these data, we concluded that p.G257R is a trafficking-deficient mutant. To confirm that the trafficking deficiency of p.G257R is specifically pathogenic, we tested three other *SCN1B* non-seizure-related polymorphic variants containing amino acid substitutions in β1B found in our cohort of patients: p.R214Q, p.S248R, p.R250T. These variants were present in each disease cohort and hence were not associated with epilepsy (Table 4). To facilitate detection of these proteins, V5-His epitope tags were inserted at their C termini, similar to p.G257RV5. 1610 cells were stably transfected and conditioned media were collected. In contrast to p.G257RV5, all three variants were detected in the conditioned media similar to wild-type β1BV5 (Fig. 9*C*). These results suggest that the lack of secretion of p.G257R is a pathogenic change and not a normal variability present in β1B polymorphisms.

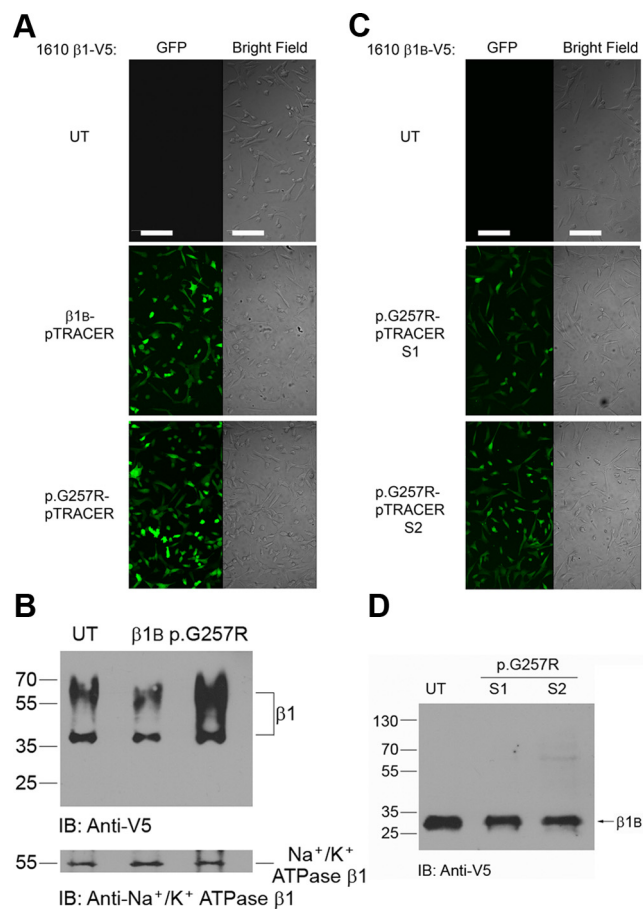Consistent with the observed intracellular retention of p.G257RV5, wild-type CGNs plated on 1610-p.G257RV5 cell

Figure 10. p.G257R does not have dominant-negative effects on wild-type β1 or β1B expression. *A*, Confirmation of expression of β1B in pTRACER-CMV2 in 1610-β1V5 cells. 1610-β1V5 cells were stably transfected with the pTRACER-CMV2 construct, fixed with 4% paraformaldehyde, and monitored for GFP fluorescence (left panels) and bright-field images (right panels), as indicated, using confocal microscopy. UT indicates untransfected cells. Scale bars, 100 μm. *B*, β1B p.G257R does not inhibit the cell surface expression of β1 or β1B. Top panel, Surface biotinylation of 1610 cells stably coexpressing V5-tagged β1 and either β1B or p.G257R. 1610-β1V5 cells (UT lane) show normal surface expression of β1. Bottom panel, Western blot of the same samples probed with anti-Na$^+$/K$^+$ ATPase β1 show equal loading of surface proteins. *C*, Confirmation of expression of p.G257R in pTRACER-CMV2 in 1610-β1BV5 cells. 1610-β1BV5 cells were stably transfected with the pTRACER-CMV2 construct, fixed with 4% paraformaldehyde, and monitored for GFP fluorescence (left panels) and bright-field images (right panels), as indicated, using confocal microscopy. UT indicates untransfected cells. Scale bars, 100 μm. *D*, p.G257R does not inhibit secretion of β1B. Conditioned media from two independent cell clones coexpressing β1BV5 and p.G257R (p.G257R S1 and S2) were collected and analyzed by Western blot with anti-V5. Conditioned media from 1610-β1BV5 cells (UT) was a positive control.

monolayers had mean neurite lengths that were indistinguishable from those plated on untransfected 1610 cells (1610-p.G257RV5, 40.87 ± 1.56 μm, vs 1610, 35.96 ± 1.63 μm; $n = 300$ and 200, respectively) and significantly shorter than CGNs plated on 1610-β1V5 (70.02 ± 2.07 μm; $n = 300$) or 1610-β1BV5 (65.89 ± 2.31 μm; $n = 300$; $p < 0.001$) (Fig. 9*D*). These results demonstrate that p.G257R is a functional null allele.

To test whether p.G257R may inhibit β1 cell surface expression via a dominant-negative function, 1610-β1V5 cells were stably transfected with cDNA encoding either β1B or p.G257R in pTRACER-CMV2. This plasmid encodes EGFP under control of a separate promoter than that used for the multiple cloning site. After stable transfection, >99% of the 1610-β1V5 cells coexpressing β1B or p.G257R showed green fluorescence, confirming β1B or p.G257R protein expression (Fig. 10*A*,*C*). Surface bioti-
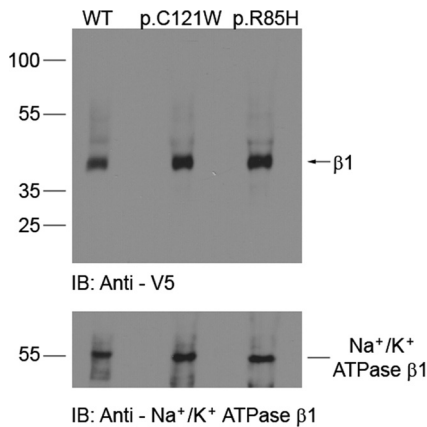
Figure 11. *SCN1B* p.C121W and p.R85H are expressed at the cell surface. Top panel, Western blot showing surface biotinylation of 1610 cells stably transfected with V5-His-tagged β1 wild-type (WT), V5-His-tagged β1 p.C121W, or V5-His-tagged β1 p.R85H. Bottom panel, Western blot of the same samples with anti-Na$^+$/K$^+$ ATPase β1 showed equal loading of surface proteins.

nylation assays were subsequently performed on 1610-β1V5 cells or 1610-β1V5 cells coexpressing either wild-type β1B or p.G257R in pTRACER-CMV2. Surface expression of β1V5 was detected by probing the Western blots with anti-V5 antibody. All lanes showed similar levels of β1V5 surface expression, indicating that coexpression of β1B or p.G257R did not interfere with β1 trafficking to the plasma membrane (Fig. 10*B*). A similar strategy was used to assess whether p.G257R functioned as a dominant negative for wild-type β1B secretion. Stably transfected 1610-β1BV5 cells were transfected with p.G257R in pTRACER-CMV2 (Fig. 10*C*). Western blots of conditioned media were probed with anti-V5 to detect wild-type β1B secretion. Conditioned media collected from 1610-β1BV5 cells were used as a positive control. Comparable levels of anti-V5-immunoreactive bands were detected in all lanes, demonstrating that p.G257R does not interfere with wild-type β1B secretion (Fig. 10*D*).

Are other *SCN1B* epilepsy-linked mutations trafficking deficient?

SCN1B p.R125C (Patino et al., 2009) and p.G257R (above) are retained intracellularly. Is this a general mechanism of *SCN1B*-linked epilepsy? To test this possibility, we expressed *SCN1B* p.C121W (Wallace et al., 2002b) and p.R85H (Xu et al., 2007) in 1610 cells and performed surface biotinylation assays as described for Figure 3. As shown in Figure 11, in contrast to p.R125C and p.G257R and in agreement with our previous study of p.C121W (Meadows et al., 2002b), both of these mutants were observed to be robustly expressed at the cell surface. Thus, at least in heterologous cells, intracellular retention resulting in a functional null phenotype is not a general mechanism of *SCN1B*-linked epilepsy.

Discussion

Despite an extensive literature demonstrating dramatic effects of β1-subunit coexpression on Na$^+$ current in heterologous systems, the major role of *SCN1B in vivo* appears to be cell adhesion (Patino and Isom, 2010). Studies with *Scn1b*-null mice show that this gene plays significant roles in promoting neuronal migration, neurite extension, and axonal fasciculation in brain and corticospinal tract (Brackenbury et al., 2008a, 2010). While many studies have shown dramatic *Scn1b*-mediated Na$^+$ current modulation in heterologous systems *in vitro* (for review, see Patino

and Isom, 2010), the observed effects of *Scn1b* deletion or mutation on Na$^+$ current *in vivo* are neuronal cell type specific and more subtle than observed in *Xenopus* oocytes or transfected cells (Chen et al., 2004; Aman et al., 2009; Brackenbury et al., 2010; Uebachs et al., 2010; Wimmer et al., 2010). It is important to consider, however, that multiplication of these small effects through synaptic networks may result in large changes in excitability *in vivo*. Na$^+$ current is required for *Scn1b*-mediated neurite outgrowth (Brackenbury et al., 2010), but we argue that *Scn1b*-mediated modulation of Na$^+$ current is not. Localization of Na$_v$1.6 to the axon initial segment is modulated by *Scn1b* and is critical for *Scn1b*-mediated neurite outgrowth in CGNs (Brackenbury et al., 2010). However, this effect is likely attributed to *Scn1b*-mediated cell-adhesive interactions and not *Scn1b*-mediated Na$^+$ current modulation. Clearly, *Scn1b* plays multifunctional signaling roles *in vivo*. A critical future experiment will be to separate the effects of *Scn1b* on Na$^+$ current modulation from those on cell adhesion to assess their relative impacts in brain *in vivo*.

The present results emphasize that understanding the physiological role of *SCN1B* in brain must include consideration of the structure and function of β1B in addition to β1. This is underappreciated in the field, as most studies have considered only β1. Our results showing that β1B is a secreted CAM expressed in embryonic brain that exerts only subtle effects on neuronal VGSC α-subunits suggest that this splice variant may play critical roles in *SCN1B* function during brain development through nonconducting cell adhesive mechanisms. Interestingly, because β1B is a secreted protein, it may play autocrine or paracrine roles in neuronal pathfinding. Deletion of β1B may make a significant contribution to the severe neurological *Scn1b*-null phenotype. This phenotype includes not only *Scn1b*-null mice but also the functional null *SCN1B* p.R125C mutation linked to Dravet syndrome in humans (Patino et al., 2009). Before the present study, all reported *SCN1B* mutations associated with human epilepsy were found to be located in the Ig domain that is shared between β1 and β1B. These results suggest that cell adhesion is clinically relevant and, importantly, that disruption of either splice variant may result in human brain disease. Novel evidence provided here demonstrates that β1B p.G257R (located in the retained intronic region unique to β1B) may be a risk factor for human epilepsy, suggesting that β1B is a critical player in brain development.

CAMs are critical for normal nervous system development and for synaptic plasticity in adulthood. Dysregulation of neural cell adhesion molecule (NCAM) expression or signaling is associated with a number of brain disorders, including depression, anxiety, bipolar disorder, and schizophrenia (for review, see Brennaman and Maness, 2010). Deletion of Nr-CAM (neuronal cell adhesion molecule) in mice results in an altered behavioral phenotype reflective of increased impulsivity (Matzel et al., 2008). Deletion of the CAM Lsamp in mice leads to heightened reactivity to novelty (Catania et al., 2008) and conditional deletion of L1-CAM in brain results in decreased anxiety-like behavior (Law et al., 2003). Epilepsy and neuropsychiatric disease have a bidirectional relationship of comorbidity (Dixon-Salazar et al., 2004; Gargus, 2006; Jacoby and Thapar, 2009; Pauli and Stefan, 2009; Spence and Schneider, 2009) and thus may share common genetic mechanisms. *SCN1B*-dependent regulation of neuronal pathfinding may be critical to abnormal brain development in both neurological and psychiatric disease. Expression of multiple *SCN1B* splice variants, including a secreted form, is also consistent with other members of the Ig superfamily of CAMs (Rougon and Hobert, 2003; Jones et al., 2009). For example, increased

expression of secreted forms of NCAM is associated with bipolar disorder and depression (Brennaman and Maness, 2010). In a similar way, modulation of β1B secretion may have pathological consequences in brain, as suggested here for β1B p.G257R.

We did not detect biochemical association of human β1B with human Na$_v$1.1, Na$_v$1.3, or Na$_v$1.5. Despite this, coexpression of Na$_v$1.3 and β1B revealed subtle changes in Na$^+$ current, similar to our previously published results with rat β1B and Na$_v$1.2 (Kazen-Gillespie et al., 2000), suggesting that β1B may associate weakly or transiently with VGSC α-subunits and play a minor current modulatory role in brain. We observed that β1B was sequestered at the cell surface by Na$_v$1.5 but not by Na$_v$1.1 or Na$_v$1.3. Thus, the association between β1B and Na$_v$1.5 may be stronger than between β1B and the tetrodotoxin-sensitive channels, in agreement with a previous study showing modulation of Na$_v$1.5 current density in heterologous cells by β1B and that a SCN1B mutation linked to Brugada syndrome disrupts the Na$^+$ current modulatory properties of β1B (Watanabe et al., 2008). In addition to heart, Na$_v$1.5 is expressed in a population of limbic neurons in brain (Hartmann et al., 1999). Differential β1B expression in specific brain areas may result in diverse effects on excitability and neurite outgrowth depending on which VGSC α-subunits are coexpressed or perhaps upregulated in response to pathology (Waxman, 2006). These data, in concert with our recent results showing specific partnering of Na$_v$1.6 and β1-subunits in cerebellum (Brackenbury et al., 2010), raise the possibility that certain VGSC α- and β-subunits form selective partnerships in excitable cells.

SCN1B p.G257R results in intracellular retention of β1B, generating a functional null cellular phenotype. This mechanism is consistent with that of p.R125C, linked to Dravet syndrome, which results in intracellular retention of β1 and, presumably, β1B as well (Patino et al., 2009). Despite this commonality, we demonstrate here that p.C121W and p.R85H are normally trafficked in heterologous cells, suggesting that intracellular retention is not a shared mechanism of SCN1B epilepsy mutations. These results agree with our previous results in heterologous cells (Meadows et al., 2002b), but contrast with β1(C121W) knock-in mice, in which p.C121W appears to be retained inside the neuron (Wimmer et al., 2010). Trafficking of this mutant subunit may differ in brain neurons compared with transfected fibroblasts. Alternatively, p.C121W may be transiently trafficked to the cell surface in both cell types, but then rapidly endocytosed due to protein misfolding or lack of cell-adhesive properties (Meadows et al., 2002b).

For p.R125C and p.G257R, retention of these subunits in the cytoplasm may inhibit signaling or trafficking of other proteins or induce cellular stress leading to neural degeneration. Thus, SCN1B gene dosage may be critical for brain disease. Heterozygous expression of one mutant and one wild-type SCN1B allele results in mild to moderate GEFS+ spectrum disorders with incomplete penetrance in human patients, with symptom severity likely depending on genetic background and/or epigenetic factors. In this sense, the pedigrees presented in our study are similar to those reported previously (Scheffer et al., 2007; Watanabe et al., 2008). In contrast, inheritance of two mutant SCN1B alleles affecting the region common to β1 and β1B and resulting in intracellular retention causes Dravet syndrome, the most severe, and sometimes fatal, disorder of the GEFS+ spectrum (Patino et al., 2009). If, as predicted by the present data, secreted β1B regulates neurite extension in developing human brain through cell-adhesive interactions, gene dosage will be critically important, as

varying levels of SCN1B expression are predicted to regulate gradients of β1B in the extracellular matrix, which may then serve as attractive or repulsive signals. The contribution of β1B to brain development is not yet known; however, our results shed new light on the role of this subunit in SCN1B function and present a fresh perspective on the biology of these multifunctional subunits.

References

Aman TK, Grieco-Calub TM, Chen C, Rusconi R, Slat EA, Isom LL, Raman IM (2009) Regulation of persistent Na current by interactions between β subunits of voltage-gated Na channels. J Neurosci 29:2027–2042.

Bourgeois S, Labuda D (2004) Dynamic allele-specific oligonucleotide hybridization on solid support. Anal Biochem 324:309–311.

Brackenbury WJ, Davis TH, Chen C, Slat EA, Detrow MJ, Dickendesher TL, Ranscht B, Isom LL (2008a) Voltage-gated Na$^+$ channel β1 subunit-mediated neurite outgrowth requires Fyn kinase and contributes to postnatal CNS development in vivo. J Neurosci 28:3246–3256.

Brackenbury WJ, Djamgoz MB, Isom LL (2008b) An emerging role for voltage-gated Na$^+$ channels in cellular migration: regulation of central nervous system development and potentiation of invasive cancers. Neuroscientist 14:571–583.

Brackenbury WJ, Calhoun JD, Chen C, Miyazaki H, Nukina N, Oyama F, Ranscht B, Isom LL (2010) Functional reciprocity between Na$^+$ channel Nav1.6 and beta1 subunits in the coordinated regulation of excitability and neurite outgrowth. Proc Natl Acad Sci U S A 107:2283–2288.

Brennaman LH, Maness PF (2010) NCAM in neuropsychiatric and neurodegenerative disorders. Adv Exp Med Biol 663:299–317.

Catania EH, Pimenta A, Levitt P (2008) Genetic deletion of Lsamp causes exaggerated behavioral activation in novel environments. Behav Brain Res 188:380–390.

Catterall WA, Goldin AL, Waxman SG (2005) International Union of Pharmacology. XLVII. Nomenclature and structure-function relationships of voltage-gated sodium channels. Pharmacol Rev 57:397–409.

Chen C, Westenbroek RE, Xu X, Edwards CA, Sorenson DR, Chen Y, McEwen DP, O'Malley HA, Bharucha V, Meadows LS, Knudsen GA, Vilaythong A, Noebels JL, Saunders TL, Scheuer T, Shrager P, Catterall WA, Isom LL (2004) Mice lacking sodium channel β1 subunits display defects in neuronal excitability, sodium channel expression, and nodal architecture. J Neurosci 24:4030–4042.

Claros MG, von Heijne G (1994) TopPred II: an improved software for membrane protein structure predictions. Comput Appl Biosci 10:685–686.

Davis TH, Chen C, Isom LL (2004) Sodium channel β1 subunits promote neurite outgrowth in cerebellar granule neurons. J Biol Chem 279:51424–51432.

Dib-Hajj SD, Waxman SG (1995) Genes encoding the β1 subunit if voltage-dependent Na$^+$ channel in rat, mouse and human condition conserved introns. FEBS Lett 377:485–488.

Dixon-Salazar TJ, Keeler LC, Trauner DA, Gleeson JG (2004) Autism in several members of a family with generalized epilepsy with febrile seizures plus. J Child Neurol 19:597–603.

Gargus JJ (2006) Ion channel functional candidate genes in multigenic neuropsychiatric disease. Biol Psychiatry 60:177–185.

Hartmann HA, Colom LV, Sutherland ML, Noebels JL (1999) Selective localization of cardiac SCN5A sodium channels in limbic regions of rat brain. Nature 2:593–595.

Isom LL, De Jongh KS, Patton DE, Reber BF, Offord J, Charbonneau H, Walsh K, Goldin AL, Catterall WA (1992) Primary structure and functional expression of the β1 subunit of the rat brain sodium channel. Science 256:839–842.

Isom LL, Scheuer T, Brownstein AB, Ragsdale DS, Murphy BJ, Catterall WA (1995) Functional co-expression of the β1 and type IIA α subunits of sodium channels in a mammalian cell line. J Biol Chem 270:3306–3312.

Jacoby A, Thapar A (2009) The contribution of seizures to psychosocial ill-health. Epilepsy Behav 15 [Suppl 1]:S41–S45.

Jones DC, Roghanian A, Brown DP, Chang C, Allen RL, Trowsdale J, Young NT (2009) Alternative mRNA splicing creates transcripts encoding soluble proteins from most LILR genes. Eur J Immunol 39:3195–3206.

Kazen-Gillespie KA, Ragsdale DS, D'Andrea MR, Mattei LN, Rogers KE, Isom LL (2000) Cloning, localization, and functional expression of sodium channel β1A subunits. J Biol Chem 275:1079–1088.

Law JW, Lee AY, Sun M, Nikonenko AG, Chung SK, Dityatev A, Schachner M, Morellini F (2003) Decreased anxiety, altered place learning, and increased CA1 basal excitatory synaptic transmission in mice with conditional ablation of the neural cell adhesion molecule L1. J Neurosci 23:10419–10432.

Lopez-Santiago LF, Meadows LS, Ernst SJ, Chen C, Malhotra JD, McEwen DP, Speelman A, Noebels JL, Maier SK, Lopatin AN, Isom LL (2007) Sodium channel SCN1B null mice exhibit prolonged QT and RR intervals. J Mol Cell Cardiol 43:636–647.

Makielski JC, Ye B, Valdivia CR, Pagel MD, Pu J, Tester DJ, Ackerman MJ (2003) A ubiquitous splice variant and a common polymorphism affect heterologous expression of recombinant human SCN5A heart sodium channels. Circ Res 93:821–828.

Malhotra JD, Kazen-Gillespie K, Hortsch M, Isom LL (2000) Sodium channel β subunits mediate homophilic cell adhesion and recruit ankyrin to points of cell-cell contact. J Biol Chem 275:11383–11388.

Malhotra JD, Koopmann MC, Kazen-Gillespie KA, Fettman N, Hortsch M, Isom LL (2002) Structural requirements for interaction of sodium channel β1 subunits with ankyrin. J Biol Chem 277:26681–26688.

Matzel LD, Babiarz J, Townsend DA, Grossman HC, Grumet M (2008) Neuronal cell adhesion molecule deletion induces a cognitive and behavioral phenotype reflective of impulsivity. Genes Brain Behav 7:470–480.

McEwen DP, Isom LL (2004) Heterophilic interactions of sodium channel beta 1 subunits with axonal and glial cell adhesion molecules. J Biol Chem 279:52744–52752.

McEwen DP, Meadows LS, Chen C, Thyagarajan V, Isom LL (2004) Sodium channel β1 subunit-mediated modulation of Nav1.2 currents and cell surface density is dependent on interactions with contactin and ankyrin. J Biol Chem 279:16044–16049.

McEwen DP, Chen C, Meadows LS, Lopez-Santiago L, Isom LL (2009) The voltage-gated Na+ channel β3 subunit does not mediate *trans* homophilic cell adhesion or associate with the cell adhesion molecule contactin. Neurosci Lett 462:272–275.

Meadows LS, Chen YH, Powell AJ, Clare JJ, Ragsdale DS (2002a) Functional modulation of human brain Nav1.3 sodium channels, expressed in mammalian cells, by auxiliary beta 1, beta 2 and beta 3 subunits. Neuroscience 114:745–753.

Meadows LS, Malhotra J, Loukas A, Thyagarajan V, Kazen-Gillespie KA, Koopman MC, Kriegler S, Isom LL, Ragsdale DS (2002b) Functional and biochemical analysis of a sodium channel β1 subunit mutation responsible for generalized epilepsy with febrile seizures plus type 1. J Neurosci 22:10699–10709.

Meisler MH, O'Brien JE, Sharkey LM (2010) Sodium channel gene family: epilepsy mutations, gene interactions and modifier effects. J Physiol 588:1841–1848.

Oh Y, Waxman SG (1994) The beta 1 subunit mRNA of the rat brain Na+ channel is expressed in glial cells. Proc Natl Acad Sci U S A 91:9985–9989.

Patino GA, Isom LL (2010) Electrophysiology and beyond: multiple roles of Na+ channel beta subunits in development and disease. Neurosci Lett 486:53–59.

Patino GA, Claes LR, Lopez-Santiago LF, Slat EA, Dondeti RS, Chen C, O'Malley HA, Gray CB, Miyazaki H, Nukina N, Oyama F, De Jonghe P, Isom LL (2009) A functional null mutation of SCN1B in a patient with Dravet syndrome. J Neurosci 29:10764–10778.

Pauli E, Stefan H (2009) Emotional and affective disorders, anxiety and personality disorders in epilepsies (in German). Nervenarzt 80:1440–1451.

Qin N, D'Andrea MR, Lubin ML, Shafaee N, Codd EE, Correa AM (2003) Molecular cloning and functional expression of the human sodium channel beta1B subunit, a novel splicing variant of the beta1 subunit. Eur J Biochem 270:4762–4770.

Remme CA, Wilde AA, Bezzina CR (2008) Cardiac sodium channel overlap syndromes: different faces of SCN5A mutations. Trends Cardiovasc Med 18:78–87.

Rougon G, Hobert O (2003) New insights into the diversity and function of neuronal immunoglobulin superfamily molecules. Annu Rev Neurosci 26:207–238.

Ruan Y, Liu N, Priori SG (2009) Sodium channel mutations and arrhythmias. Nat Rev Cardiol 6:337–348.

Scheffer IE, Harkin LA, Grinton BE, Dibbens LM, Turner SJ, Zielinski MA, Xu R, Jackson G, Adams J, Connellan M, Petrou S, Wellard RM, Briellmann RS, Wallace RH, Mulley JC, Berkovic SF (2007) Temporal lobe epilepsy and GEFS+ phenotypes associated with SCN1B mutations. Brain 130:100–109.

Spence SJ, Schneider MT (2009) The role of epilepsy and epileptiform EEGs in autism spectrum disorders. Pediatr Res 65:599–606.

Thompson JD, Higgins DG, Gibson TJ (1994) CLUSTAL W: improving the sensitivity of progressive multiple sequence alignment through sequence weighting, position-specific gap penalties and weight matrix choice. Nucleic Acids Res 22:4673–4680.

Uebachs M, Opitz T, Royeck M, Dickhof G, Horstmann MT, Isom LL, Beck H (2010) Efficacy loss of the anticonvulsant carbamazepine in mice lacking sodium channel β subunits via paradoxical effects on persistent sodium current. J Neurosci 30:8489–8501.

von Heijne G (1992) Membrane protein structure prediction. Hydrophobicity analysis and the positive-inside rule. J Mol Biol 225:487–494.

Wallace RH, Scheffer IE, Parasivam G, Barnett S, Wallace GB, Sutherland GR, Berkovic SF, Mulley JC (2002) Generalized epilepsy with febrile seizures plus: mutation of the sodium channel subunit SCN1B. Neurology 58:1426–1429.

Watanabe H, Koopmann TT, Le Scouarnec S, Yang T, Ingram CR, Schott JJ, Demolombe S, Probst V, Anselme F, Escande D, Wiesfeld AC, Pfeufer A, Kääb S, Wichmann HE, Hasdemir C, Aizawa Y, Wilde AA, Roden DM, Bezzina CR (2008) Sodium channel beta1 subunit mutations associated with Brugada syndrome and cardiac conduction disease in humans. J Clin Invest 118:2260–2268.

Watanabe H, Darbar D, Kaiser DW, Jiramongkolchai K, Chopra S, Donahue BS, Kannankeril PJ, Roden DM (2009) Mutations in sodium channel β1- and β2-subunits associated with atrial fibrillation. Circ Arrhythm Electrophysiol 2:268–275.

Waxman SG (2006) Ions, energy and axonal injury: towards a molecular neurology of multiple sclerosis. Trends Mol Med 12:192–195.

Wimmer VC, Reid CA, Mitchell S, Richards KL, Scaf BB, Leaw BT, Hill EL, Royeck M, Horstmann MT, Cromer BA, Davies PJ, Xu R, Lerche H, Berkovic SF, Beck H, Petrou S (2010) Axon initial segment dysfunction in a mouse model of genetic epilepsy with febrile seizures plus. J Clin Invest 120:2661–2671.

Xu R, Thomas EA, Gazina EV, Richards KL, Quick M, Wallace RH, Harkin LA, Heron SE, Berkovic SF, Scheffer IE, Mulley JC, Petrou S (2007) Generalized epilepsy with febrile seizures plus-associated sodium channel beta1 subunit mutations severely reduce beta subunit-mediated modulation of sodium channel function. Neuroscience 148:164–174.